Available online at www.sciencedirect.com
ScienceDirect
Coordination Chemistry Reviews 251 (2007) 2311–2333
COORDINATION CHEMISTRY REVIEWS
www.elsevier.com/locate/ccr

Review

Synthesis and structural characterization of silver(I) double and multiple salts containing the acetylenediide dianion

Thomas Chung Wai Mak *, Xiao-Li Zhao, Quan-Ming Wang [1], Guo-Cong Guo [2]

Department of Chemistry and Center of Novel Functional Molecules, The Chinese University of Hong Kong, Shatin, New Territories, Hong Kong SAR, PR China

Received 30 September 2006; accepted 6 November 2006
Available online 12 November 2006

Dedicated to Prof. Sunney Ignatius Chan on the occasion of his 70th birthday.

Contents

* Corresponding author. Tel.: +852 2609 6279; fax: +852 2603 5057.
E-mail address: tcwmak@cuhk.edu.hk (T.C.W. Mak).
[1] Present address: Department of Chemistry, College of Chemistry and Chemical Engineering, Xiamen University, Xiamen 361005, PR China.
[2] Present address: State Key Laboratory of Structural Chemistry, Fujian Institute of Research on the Structure of Matter, Chinese Academy of Sciences, Fuzhou, Fujian 350002, PR China.

doi:10.1016/j.ccr.2006.11.001

Abstract

A large family of crystalline compounds with silver acetylenediide (Ag_2C_2) as a component have been synthesized and characterized. In most cases the C_2^{2-} species is enclosed in a silver(I) polyhedron of 6–10 vertices, which may be symbolized as $C_2@Ag_n$ (n = 6–10). In the present review, emphasis is laid on our systematic studies in the controlled generation and supramolecular assembly of $C_2@Ag_n$ polyhedra to form discrete molecules and higher-dimensional aggregates with the aid of co-existing anions and ancillary ligands.

Keywords: Acetylenediide; Acetylide; Argentophilicity; Coordination network; Ethynediide; Double salt; Multiple salt; Silver(I) complex; Supramolecular assembly

1. Introduction

The Group 11 and Group 12 metal acetylenediides (Cu_2C_2, Ag_2C_2, Au_2C_2, ZnC_2, CdC_2, $Hg_2C_2{\cdot}H_2O$ and HgC_2) exhibit properties that are characteristic of covalent polymeric solids, but their tendency to detonate upon mechanical shock and insolubility in most solvents present serious difficulties in structural characterization. Six decades ago, it was discovered that silver acetylenediide (or ethynediide), commonly known as silver acetylide or silver carbide, can be dissolved in a concentrated aqueous solution of silver nitrate to yield the crystalline double salt $Ag_2C_2{\cdot}6AgNO_3$ [1a]. Soon afterwards, the preparation of a series of double salts of the general formula $Ag_2C_2{\cdot}m$AgX, where X = Cl, I, NO_3, H_2AsO_4 or $1/2EO_4$ (E = S, Se, Cr or W) and m is the molar ratio, was reported [1a,1b]. The first X-ray analysis in 1954 of $Ag_2C_2{\cdot}6AgNO_3$ revealed a rhombohedral Ag_8 cage with an encapsulated acetylenediide dianion, but the dumbbell-like C_2^{2-} moiety was wrongly aligned along the crystallographic 3-axis [1c]. Re-determination of the structure in 1990 showed that the C_2^{2-} species lies perpendicular to the 3-axis owing to orientational disorder [1d].

In 1997, we embarked on a systematic study on the synthesis and characterization of silver(I) complexes containing Ag_2C_2 as a constituent. The accumulated results demonstrated that a common feature to this class of compounds is the existence of polynuclear silver(I) aggregates with embedded C_2^{2-} species, which generally take the shape of convex polyhedra and can be symbolized as $C_2@Ag_n$ (n = 6–10). In these compounds, the Ag···Ag, Ag–C and C–C bond distances fall in the range of 2.7–3.4, 2.1–2.8 and 1.1–1.2 Å, respectively.

The present article summarizes the research findings of our group on the generation, structural characterization, and attempted modification of the $C_2@Ag_n$ moieties, as well as their utilization as versatile building blocks for supramolecular assembly.

2. Argentophilicity

Normally, two closed-shell metal cations would be expected to repel each other. However, strong metal–metal attraction exists in a large number of inorganic and organometallic complexes, and the term "metallophilicity" has been coined to describe such interactions [2]. In particular, concrete experimental evidence has accrued on the association between d^{10} metal ions, especially those of the Group 11 coinage metals. With regard to aurophilicity, defined as the propensity for aggregation of Au(I), electron correlation, relativity effects and the gold–phosphine interaction combine to produce an effective gold configuration closer to $5d^9$ than $5d^{10}$. The strength of aurophilic interaction (7–11 kcal mol^{-1}) is comparable to that of a typical hydrogen bond [3]. As to analogous cuprophilicity and argentophilicity exhibited by the lighter congeners, the majority of short metal–metal contacts found in Ag^I/Cu^I complexes are associated with ligand bridged, network-restricted, or coulombic effects [4]. However, theoretical evidence has been provided for transannular metal–metal interactions in dinuclear coinage metal compounds [5]. There are now many examples of ligand-unsupported Ag–Ag contacts based on X-ray structural determinations [6]. Furthermore, convincing spectroscopic evidence has been gathered to substantiate the significance of argentophilicity and cuprophilicity [7].

3. Silver(I) double/multiple salts containing Ag_2C_2

The structure of Ag_2C_2 is unknown, but it has been assumed to be a polymeric solid involving both σ and π bonding of the C_2 unit to neighboring silver(I) atoms, which may account for its insolubility in common solvents. The mechanism of dissolution of Ag_2C_2 in a concentrated aqueous solution containing one or more soluble silver(I) salts is not clearly understood, but it is conceivable that argentophilicity provides the driving force to transform polymeric Ag_2C_2 to labile $C_2@Ag_n$ species. The water-soluble silver salts that we have employed in our synthetic studies include silver fluoride, silver perchlorate, silver nitrate, silver tetrafluoroborate, silver triflate and silver trifluoroacetate, the last being the most versatile.

CAUTION: Thoroughly dried Ag_2C_2 detonates easily upon mechanical shock, and only a small quantity of freshly prepared sample should be used in any chemical reaction. Excess amount can be disposed of via slow decomposition in an alkaline solution. To ensure safety, we used moist Ag_2C_2 in all preparations.

The chemical formulae of most of the compounds described in this review are expressed in one-line formulae such as kAgX·lAgY·mAgZ·nL, where k, l, m and n are the molar ratios, X, Y and Z are mono-anions, and L is a solvent molecule often serving as a neutral terminal ligand. Most of these double/multiple salts of silver(I) exhibit 1D, 2D or 3D network structures in the solid state. When the compound contains organic cations and Ag_2C_2-containing anions, such as in $[Et_4N]_6\{(Ag_2C_2)_2(AgCF_3CO_2)_8(CF_3CO_2)_3(H_2O)_2\}_2$, the cation is enclosed in square brackets, and the remaining anionic components are grouped together in the formula. Curved brackets and italicized subscript n are used to indicate polymeric structures, as in $\{Ag_2C_2{\cdot}4AgC_2F_5CO_2{\cdot}[bppH]C_2F_5CO_2\}_n$.

Each compound mentioned for the first time is highlighted in bold format.

3.1. Double salts

Our study began with the double salt **Ag_2C_2·8AgF**, which was obtained in quantitative yield by dissolving Ag_2C_2 in a concentrated aqueous solution of AgF [8]. Structural analysis revealed the presence of an exohedral silver(I) atom attached, without ligand bridging, to the apex of a cationic Ag_9 cage, whose cavity is filled by an ordered acetylenediide dianion. The Ag_9 cage can be described as a capped square antiprism of approximate C_{4v} symmetry in which all four edges of the expanded capped face have been cleaved (Fig. 1a). Adjacent [Ag_9]Ag moieties are bridged by fluoride ions to form a 3D framework (Fig. 1b). The measured C–C bond length of 1.175(7) Å indicates that the encapsulated acetylenediide dianion retains its triple-bond character, as confirmed by laser Raman absorption at 2104.5 and 2168.6 cm^{-1} in the $\Delta\nu$ (C≡C) region.

In **Ag_2C_2·2AgClO$_4$·2H$_2$O**, the building unit is a C_2@Ag_6 octahedron (Fig. 1c) [9]. Silver cages of this type share vertices to generate a cationic layer structure between which the disordered perchlorate ions are accommodated, so that the crystal structure may be considered as a stack of alternate conducting and insulating layers (Fig. 1d).

Double salts of the general formula Ag_2C_2·mAgNO$_3$ (m = 1, 5, 5.5 and 6) have been synthesized under different reaction conditions [1d,10]. **Ag_2C_2·6AgNO$_3$**, the most stable phase, can be easily prepared by dissolving Ag_2C_2 in a concentrated aqueous solution of $AgNO_3$ at room temperature. As noted previously, the encapsulated C_2^{2-} is disordered about a crystallographic three-fold axis that bisects the C≡C bond and passes through two opposite corners of the elongated Ag_8 rhombohedron (Fig. 2a). At 80 °C, **Ag_2C_2·5.5AgNO$_3$·0.5H$_2$O** co-crystallizes with Ag_2C_2·6AgNO$_3$. The Ag_7 cage in Ag_2C_2·5.5AgNO$_3$·0.5H$_2$O is a monocapped octahedron with four lengthened edges, in which the acetylenediide dianion is fully encapsulated and directed toward the capping atom (Fig. 2b). Crystalline **Ag_2C_2·5AgNO$_3$** was obtained serendipitously as a mixed product together with Ag_2C_2·6AgNO$_3$ from the addition of $AgNO_3$ to a solution of Ag_2C_2 in CF_3CO_2Ag at 80 °C. The role played by CF_3CO_2Ag in this instance is not clear. The Ag_7 cage that accommodates the acetylenediide dianion in Ag_2C_2·5AgNO$_3$ can be described as a monocapped trigonal prism of imposed symmetry C_2, with lengthening of two opposite edges of its expanded capped face, and the capping atom is asymmetrically positioned owing to two-fold disorder about the 2-axis (Fig. 2c). In Ag_2C_2·6AgNO$_3$, Ag_2C_2·5.5AgNO$_3$·0.5H$_2$O and Ag_2C_2·5AgNO$_3$, the discrete silver(I) polyhedra are inter-linked by nitrate ions. **Ag_2C_2·AgNO$_3$** was obtained by hydrothermal

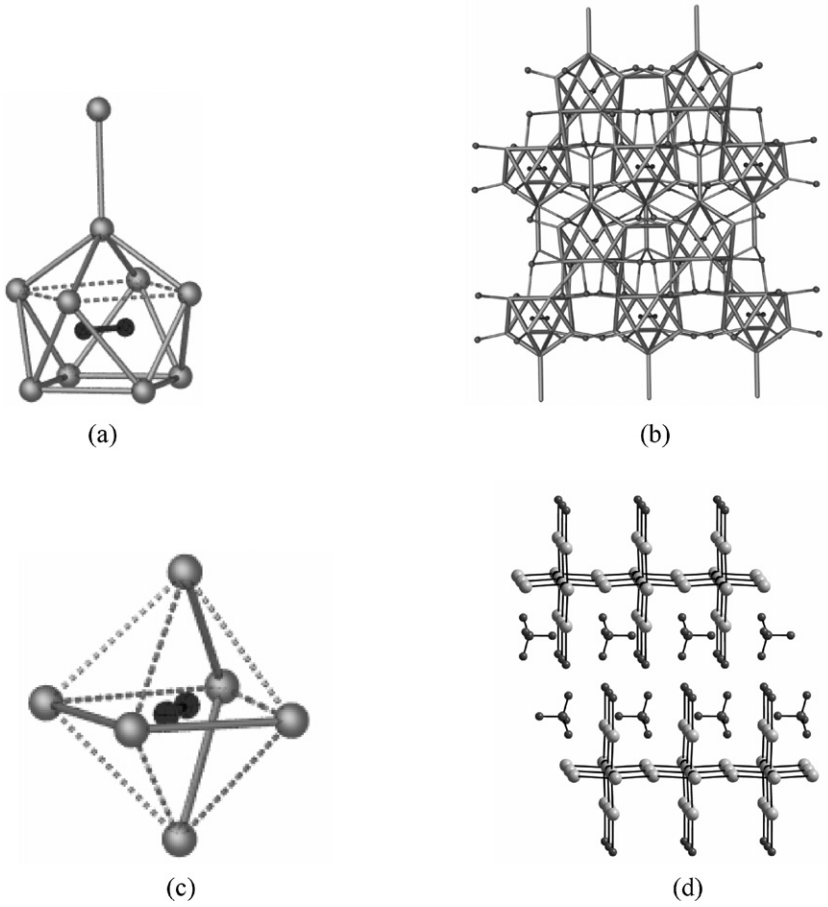

Fig. 1. (a) The C_2@[Ag_9]Ag building unit in Ag_2C_2·8AgF. (b) 3D structure of Ag_2C_2·8AgF generated from fluoride-bridged C_2@[Ag_9]Ag moieties [8]. (c) The C_2@Ag_6 building unit in Ag_2C_2·2AgClO$_4$·2H$_2$O. (d) Crystal structure of Ag_2C_2·2AgClO$_4$·2H$_2$O viewed along the c-axis [9].

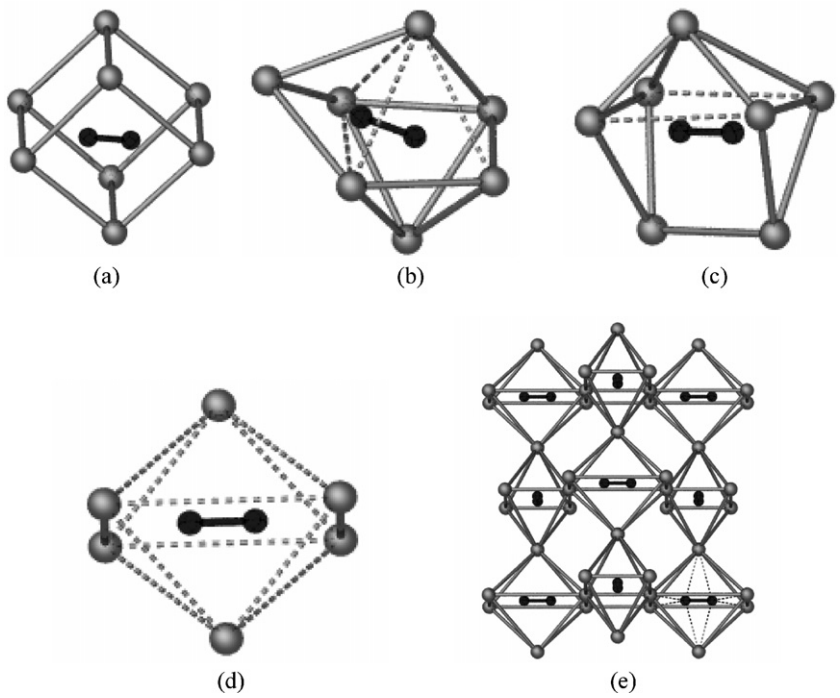

Fig. 2. The $C_2@Ag_n$ building unit in (a) $Ag_2C_2{\cdot}6AgNO_3$, (b) $Ag_2C_2{\cdot}5.5AgNO_3{\cdot}0.5H_2O$, (c) $Ag_2C_2{\cdot}5AgNO_3$ and (d) $Ag_2C_2{\cdot}AgNO_3$. (e) Stack of slabs in $Ag_2C_2{\cdot}AgNO_3$ [10].

synthesis at 105 °C. The silver(I) octahedra each enclosing a C_2^{2-} species (Fig. 2d) are connected by linking their equatorial edges to form a slab (Fig. 2e), and sharing of the remaining apices of such slabs leads to a 3D cationic network. The disordered nitrate ions are located inside the square channels generated from the linkage of silver octahedra.

When silver perfluoro-dicarboxylates ($AgO_2C(CF_2)_nCO_2Ag$; $n = 2, 3$) were employed to dissolve Ag_2C_2, two double salts **$Ag_2C_2{\cdot}3AgO_2CCF_2CF_2CO_2Ag{\cdot}7H_2O$** and **$Ag_2C_2{\cdot}4AgO_2CCF_2CF_2CF_2CO_2Ag{\cdot}17.5H_2O$** were obtained [11]. The building unit in $Ag_2C_2{\cdot}3AgO_2CCF_2CF_2CO_2Ag{\cdot}7H_2O$ is a crown-like $C_2@Ag_7$ cage (Fig. 3a). These cages are connected by tetrafluorosuccinate ligands to form a zigzag chain (Fig. 3b), and such chains are further linked by the carboxylate groups of other tetrafluorosuccinate ligands to generate layers and eventually a 3D network. The fundamental building unit of $Ag_2C_2{\cdot}4AgO_2CCF_2CF_2CF_2CO_2Ag{\cdot}17.5H_2O$ is a square-antiprismatic $C_2@Ag_8$ cage (Fig. 3c), and such polyhedra are connected by hexafluoroglutarate ligands to form a layer structure (Fig. 3d).

A partially open $C_2@Ag_7$ cage in the shape of a basket (Fig. 3e) is found in the double salt **$Ag_2C_2{\cdot}6AgO_2CCHF_2$** [12]. The basket-like cages are interconnected by difluoroacetate ligands to form a layer (Fig. 3f), which are further connected by difluoroacetate ligands through another silver(I) atom to form a 3D network.

3.2. Triple salts

The novel triple salt **$Ag_2C_2{\cdot}AgF{\cdot}4AgCF_3SO_3{\cdot}CH_3CN$** was obtained by dissolving Ag_2C_2 in an aqueous solution of silver trifluoromethanesulfonate (triflate) and silver tetrafluoroborate in the presence of acetonitrile [13]. The original purpose of adding $AgBF_4$ was to increase the silver(I) concentration to promote the dissolution of Ag_2C_2. The experimental result indicates that $AgBF_4$ plays a key role in the formation of the triple salt by functioning as a suitable precursor of AgF. The gradual release of fluoride from tetrafluoroborate induces the crystallization of the triple salt, as using AgF directly in the preparation invariably leads to formation of the thermodynamically stable $Ag_2C_2{\cdot}8AgF$. The isomorphous triple salt **$Ag_2C_2{\cdot}AgF{\cdot}4AgCF_3SO_3{\cdot}C_2H_5CN$** was prepared in a similar manner by employing C_2H_5CN instead of CH_3CN.

The crystal structure of $Ag_2C_2{\cdot}AgF{\cdot}4AgCF_3SO_3{\cdot}CH_3CN$ is constructed from a $C_2@Ag_7$ cage in the shape of a monocapped trigonal prism and a $Ag_6(\mu_3\text{-}F)(\mu_3\text{-}CF_3SO_3)_2$ capsule (Fig. 4a and b). These two kinds of building units share Ag···Ag edges to form a honeycomb-like host layer, whose hexagonal voids are filled with triflate guests (Fig. 4c). The neutral ligand CH_3CN is terminally coordinated to the capping silver atom of the $C_2@Ag_7$ cage, and it can be readily substituted by C_2H_5CN to form the isomorphous complex $Ag_2C_2{\cdot}AgF{\cdot}4AgCF_3SO_3{\cdot}C_2H_5CN$ with its layer structure kept intact [13].

$2Ag_2C_2{\cdot}AgF{\cdot}9AgNO_3{\cdot}H_2O$ was prepared by dissolving Ag_2C_2 in an aqueous solution of $AgNO_3$ and $AgBF_4$, the latter serving as a precursor of AgF [14]. Its crystal structure contains two kinds of monocapped trigonal prismatic $C_2@Ag_7$ cages, with the capping atom occurring on one triangular face or one rectangular face. These two kinds of cages each forms a zigzag chain through bridging by the nitrate ions. The chains are arranged alternately, and the fluoride and nitrate ions inter-link them to form a layer (Fig. 5a); adjacent layers being related by a 2_1 screw axis are interconnected by water ligands and nitrate ions to construct a 3D network.

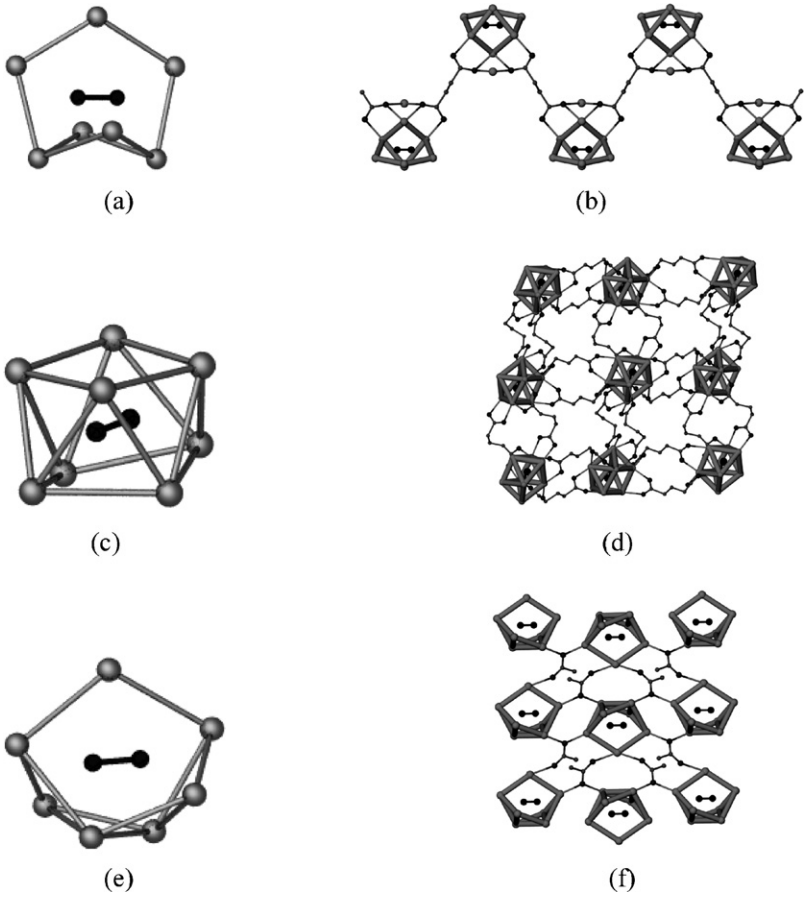

Fig. 3. (a) The crown-like Ag_7 cage enclosing an acetylenediide species in $Ag_2C_2{\cdot}3AgO_2CCF_2CF_2CO_2Ag{\cdot}7H_2O$. (b) Zigzag chain made up of $C_2@Ag_7$ linked through tetrafluorosuccinate anions in $Ag_2C_2{\cdot}3AgO_2CCF_2CF_2CO_2Ag{\cdot}7H_2O$ [11]. (c) Square-antiprismatic $C_2@Ag_8$ in $Ag_2C_2{\cdot}4AgO_2CCF_2CF_2CF_2CO_2Ag{\cdot}17.5H_2O$. (d) Layer structure of $Ag_2C_2{\cdot}4AgO_2CCF_2CF_2CF_2CO_2Ag{\cdot}17.5H_2O$ [11]. (e) Basket-like $C_2@Ag_7$ silver(I) cage in $Ag_2C_2{\cdot}6AgO_2CCHF_2$. (f) 2D network in $Ag_2C_2{\cdot}6AgO_2CCHF_2$ generated from $C_2@Ag_7$ polyhedra connected by bridging difluoroacetate ligands [12].

When tetrafluorosuccinate together with $AgNO_3$ were used to dissolve Ag_2C_2, **$2Ag_2C_2{\cdot}6AgO_2CCF_2CF_2CO_2Ag{\cdot}AgNO_3{\cdot}12H_2O$** was obtained [11]. Its structure consists of two types of silver(I) cages, namely a distorted pentagonal bipyramidal $C_2@Ag_7$ and a monocapped pentagonal bipyramidal $C_2@Ag_8$. These two kinds of cages are linked by tetrafluorosuccinate ions to generate a 3D framework (Fig. 5b).

3.3. Quadruple salt

Incorporation of AgCN and Ag_2C_2 with CF_3CO_2Ag and $AgBF_4$ into a crystalline lattice generated the first quadruple silver(I) salt **$2Ag_2C_2{\cdot}3AgCN{\cdot}15CF_3CO_2Ag{\cdot}2AgBF_4{\cdot}9H_2O$** containing four different anions [15]. It exhibits an interesting nanoscale columnar structure (Fig. 6a and b), which is built up

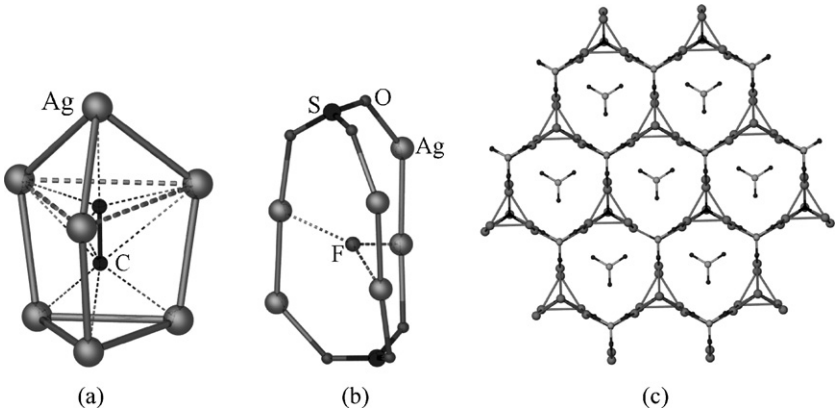

Fig. 4. (a) Monocapped trigonal prismatic $C_2@Ag_7$ in $Ag_2C_2{\cdot}AgF{\cdot}4AgCF_3SO_3{\cdot}CH_3CN$. (b) $Ag_6(\mu_3\text{-}F)(\mu_3\text{-}CF_3SO_3)_2$ capsule generated from bridging of the Ag···Ag edges of three adjacent $C_2@Ag_7$ cages by a μ_3-fluoride and two μ_3-triflates. (c) Honeycomb-like host layer in the isomorphous complexes $Ag_2C_2{\cdot}AgF{\cdot}4AgCF_3SO_3{\cdot}CH_3CN$ and $Ag_2C_2{\cdot}AgF{\cdot}4AgCF_3SO_3{\cdot}C_2H_5CN$, with triflate guests occupying the hexagonal voids [13].

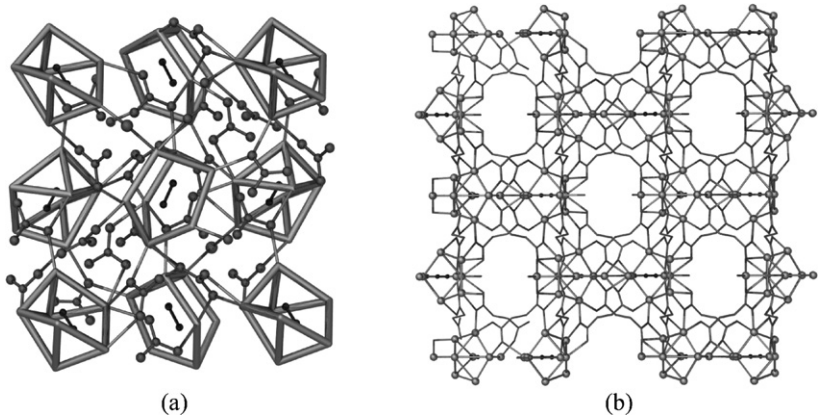

Fig. 5. (a) One layer viewed along the *c* direction in $2Ag_2C_2{\cdot}AgF{\cdot}9AgNO_3{\cdot}H_2O$ [14]. (b) Crystal structure of $2Ag_2C_2{\cdot}6AgO_2CCF_2CF_2CO_2Ag{\cdot}AgNO_3{\cdot}12H_2O$ viewed along the *b* direction [11].

from three kinds of fundamental units: **A**, **B** and **C** (Fig. 6c). Unit **A** is a double cage made of 13 silver(I) atoms and 2 encapsulated acetylenediide species, which can be viewed as 2 C_2-related bicapped trigonal prismatic $C_2@Ag_8$ polyhedra sharing a triangular face. Motif **B** $[Ag_4CN]$ is a cyanide-bridged tetra-silver(I) fragment located at a site of symmetry C_2. Motif **C** is a centrosymmetric hexa-silver(I) moiety $[Ag_6(CN)_2]$ with three pairs of silver(I) atoms side-on bridged by two ordered cyanides, each being coordinated to four silver(I) atoms. Structural units **A**, **B** and **C** are inter-linked through 7.5 independent bridging trifluoroacetate groups to generate the fascinating columnar structure.

3.4. Influence of solvent on the formation of Ag_2C_2-containing silver(I) salts

A series of silver(I) double salts were isolated by dissolving Ag_2C_2 in a concentrated aqueous solution of R_FCO_2Ag ($R_F = CF_3$, C_2F_5) and $AgBF_4$. The influence of different ancil-

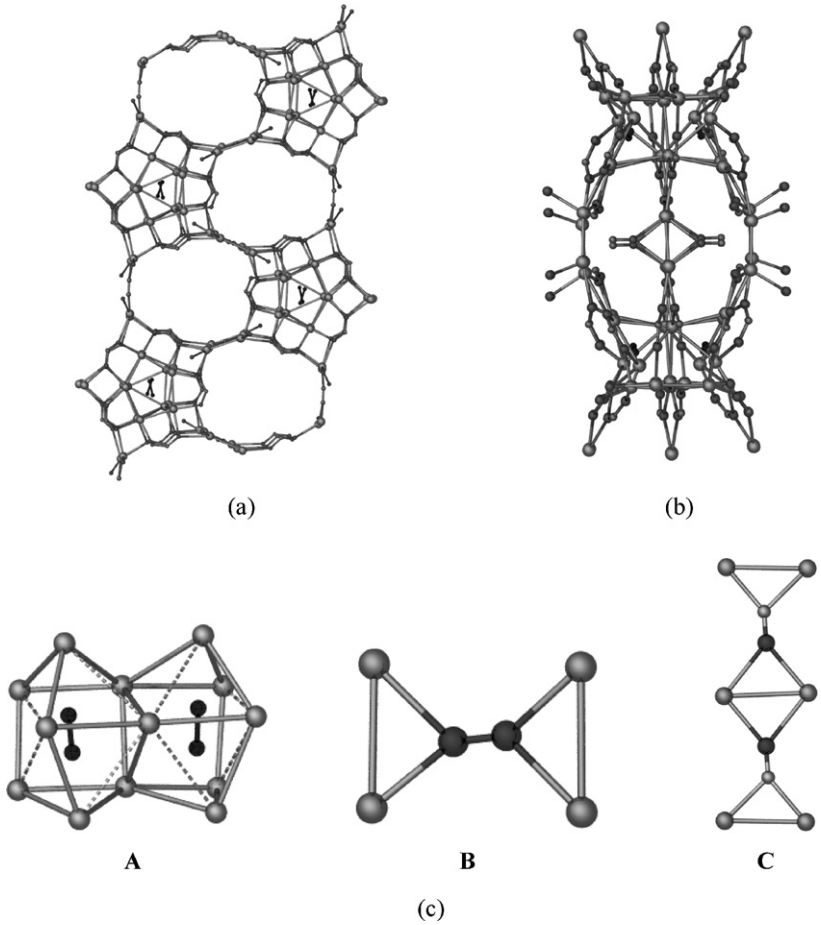

Fig. 6. (a) An elliptic column viewed approximately in the [1 0 1] direction in $2Ag_2C_2{\cdot}3AgCN{\cdot}15CF_3CO_2Ag{\cdot}2AgBF_4{\cdot}9H_2O$. (b) Oval cross-section of the elliptic column viewed along the *c* direction. (c) Structure fragments $(C_2)_2@Ag_{13}$, $[Ag_4CN]$ and $[Ag_6CN_2]$ in the construction of the quadruple salt [15].

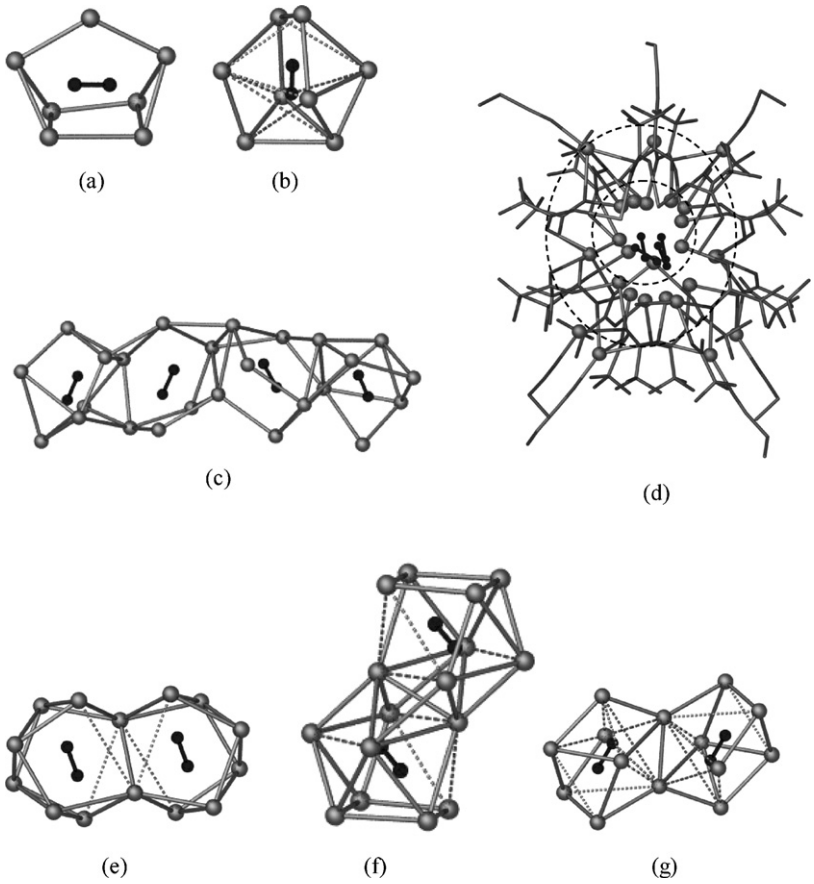

Fig. 7. The $C_2@Ag_n$ building unit in (a) $2Ag_2C_2{\cdot}12CF_3CO_2Ag{\cdot}5H_2O$, (b) $Ag_2C_2{\cdot}6CF_3CO_2Ag{\cdot}3CH_3CN$, (c) $4Ag_2C_2{\cdot}23CF_3CO_2Ag{\cdot}7C_2H_5CN{\cdot}2.5H_2O$, (e) $Ag_2C_2{\cdot}10C_2F_5CO_2Ag{\cdot}9.5H_2O$, (f) $Ag_2C_2{\cdot}9C_2F_5CO_2Ag{\cdot}3CH_3CN{\cdot}H_2O$ and (g) $Ag_2C_2{\cdot}6C_2F_5CO_2Ag{\cdot}2C_2H_5CN$, respectively. (d) Structure of $4Ag_2C_2{\cdot}23CF_3CO_2Ag{\cdot}7C_2H_5CN{\cdot}2.5H_2O$ viewed along the *a* direction, showing a cross-section of the double-walled silver column [16].

lary solvent ligands such as H_2O, CH_3CN and C_2H_5CN on the crystallization process was explored [16].

$2Ag_2C_2{\cdot}12CF_3CO_2Ag{\cdot}5H_2O$ consists of two almost identical $C_2@Ag_7$ cages in the independent unit, each having the shape of a basket with a square base (Fig. 7a). The $C_2@Ag_7$ cages are connected to each other through μ-trifluoroacetate bridges to generate a layer, and such layers are further linked by other silver(I) atoms through trifluoroacetate ions to give a 3D network. When CH_3CN is present, the adduct **$Ag_2C_2{\cdot}6CF_3CO_2Ag{\cdot}3CH_3CN$** crystallizes, whose building unit is a distorted triangulated dodecahedron with an embedded C_2^{2-} species (Fig. 7b). The dodecahedra share edges to generate a chain-like structure. These composite chains are inter-linked to each other to construct a 2D network. Replacement of CH_3CN with C_2H_5CN resulted in the formation of **$4Ag_2C_2{\cdot}23CF_3CO_2Ag{\cdot}7C_2H_5CN{\cdot}2.5H_2O$**, which features a double-walled silver column whose inner core is constructed from the fusion of four different kinds of irregular polyhedra: two monocapped trigonal prisms, a basket with an Ag_4 base, and a severely distorted pentagonal bipyramid (Fig. 7c). The inner core of the double-walled column is linked by bridging trifluoroacetate ligands to seven independent silver(I) atoms, each being coordinated by one terminal C_2H_5CN ligand, which form the outer wall. All 31 silver(I) centers in the independent unit that constitute the 1D motif are surrounded by hydrophobic C_2H_5CN and CF_3 groups, which prevent further aggregation of such motifs to generate a higher-dimensional network (Fig. 7d). In the series $2Ag_2C_2{\cdot}12CF_3CO_2Ag{\cdot}5H_2O$, $Ag_2C_2{\cdot}6CF_3CO_2Ag{\cdot}3CH_3CN$ and $4Ag_2C_2{\cdot}23CF_3CO_2Ag{\cdot}7C_2H_5CN{\cdot}2.5H_2O$, the dimensionality of the crystal structures decreases in the order of ancillary solvent ligands H_2O, CH_3CN and C_2H_5CN. Single-crystal X-ray analysis of **$Ag_2C_2{\cdot}10C_2F_5CO_2Ag{\cdot}9.5H_2O$** revealed a centrosymmetric $(C_2)_2@Ag_{14}$ double cage, which can be considered as two $C_2@Ag_8$ square antiprisms sharing an edge (Fig. 7e). Twelve pentafluoropropionate (pfp) ligands are coordinated around such a double cage to form a fundamental building unit, and such units are further connected by $[Ag_2(pfp)_2]$ bridges to generate an infinite chain. The chains are further cross-linked through two other $[Ag_2(pfp)_2]$ bridges at different orientations to form a 2D network. Identical layers are stacked with $[Ag_2(pfp)_2]$ fragments pillared between adjacent layers to form a 3D networks. The bulky tails of pfp ligands are located in these channels. When the terminally coordinated ligand acetonitrile was included in the crystallization process that yielded $Ag_2C_2{\cdot}10C_2F_5CO_2Ag{\cdot}9.5H_2O$, **$Ag_2C_2{\cdot}9C_2F_5CO_2Ag{\cdot}3CH_3CN{\cdot}H_2O$** was isolated. The building unit in this complex is a double cage formed by two inversion-related $C_2@Ag_9$ polyhedra sharing an edge; each component polyhedron can be described as a monocapped

square antiprism with one silver(I) atom capping the top face (Fig. 7f). The $(C_2)_2@Ag_{16}$ double cage is surrounded by pfp ligands, acetonitrile and water ligands, which prevent further linkage between units, and a unique discrete supermolecule forms as a result. **$Ag_2C_2{\cdot}6C_2F_5CO_2Ag{\cdot}2C_2H_5CN$** was obtained in the presence of propionitrile during crystallization. The structure features a centrosymmetric $(C_2)_2@Ag_{14}$ double cage with each component single cage taking the shape of a distorted dodecahedron (Fig. 7g), and the double cages are bridged by pfp ligands to form a 1D structure. As the chain is surrounded by terminal propionitrile ligands and C_2F_5 groups, further linkage to construct a 2D or 3D network is precluded. For the six compounds mentioned above, when nitrile (CH_3CN or C_2H_5CN) was not added to the aqueous solution in crystallization, a hydrated compound was isolated. As water ligands and lattice water molecules readily occupy voids in the structure, a 3D network is generated via bridging perfluoroalkylcarboxylates. When CH_3CN or C_2H_5CN participates in the crystallization process, its coordination to the peripheral silver atoms causes steric hindrance that prevents network assembly in three dimensions.

3.5. Crown ether-directed assembly of silver(I) aggregates

To obtain discrete molecules and infinite chains, crown ethers were employed to install protective cordons around the $C_2@Ag_n$ moiety that function as blocking groups or terminal stoppers. From similar silver(I) starting materials, various crystalline double salts have been isolated under the structure-directing influence of different crown ethers: 12C4, 15C5, benzo-15C5 and 18C6 [17].

$[(Ag_2C_2)(CF_3CO_2Ag)_5(15C5)_2(H_2O)]{\cdot}3H_2O$ with a sandwich structure can be obtained from an aqueous solution containing Ag_2C_2, $AgCF_3CO_2$ and 15C5. The discrete $C_2@Ag_7$ moiety in $[(Ag_2C_2)(CF_3CO_2Ag)_5(15C5)_2(H_2O)]{\cdot}3H_2O$ is a pentagonal bipyramid, with four equatorial edges bridged by $CF_3CO_2^-$ groups while the two apical silver atoms are each attached to a 15C5 ligand. In this discrete molecule, one equatorial silver atom is coordinated by a monodentate $CF_3CO_2^-$ and another by a water ligand (Fig. 8a).

When a smaller crown ether 12C4 is employed in place of 15C5 to form **$[Ag(12C4)_2]\{(Ag_2C_2)(AgCF_3CO_2)_8(CF_3CO_2)(12C4)_2(H_2O)_3\}{\cdot}H_2O$** not only is the sandwich unit retained but additional host–guest interaction also occurs in the crystal structure. The aggregate is composed of a $[Ag(12C4)_2]^+$ cation and a triangulated dodecahedral $C_2@Ag_8$ moiety (Fig. 8b). In $[Ag(12C4)_2]^+$, the coordination geometry at the silver(I) center is a distorted square antiprism formed by eight oxygen atoms of two 12C4 ligands. Moieties of the $\{C_2@Ag_8(12C4)_2(CF_3CO_2)_7\}^-$ type are connected through the $[Ag_2(CF_3CO_2)_2]$ linkages to generate a winding, snake-like anionic chain, while the $[Ag(12C4)_2]^+$ ions occupy the concave cavities in the inter-chain region.

When benzo-15C5 was used in the reaction, **$[(Ag_2C_2)(AgCF_3CO_2)_5(benzo\text{-}15C5)(H_2O)_2]{\cdot}0.5H_2O$** crystallized as the product. The steric influence of the benzene ring along with the anticipated silver(I)–aromatic interaction affect the assembly process, leading to the formation of a 1D poly-

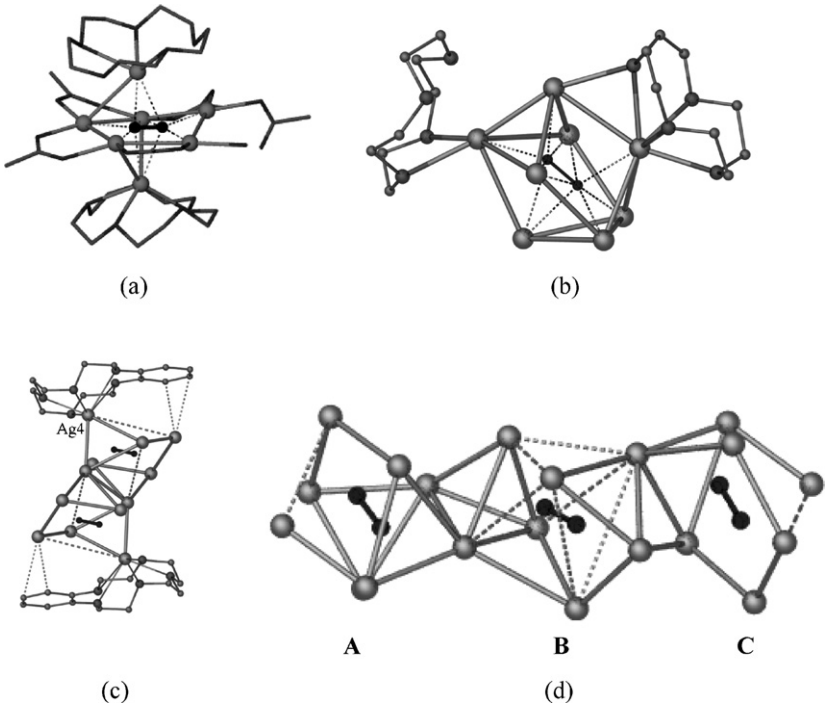

Fig. 8. (a) Crown-sandwiched structure of the discrete molecule in $[(Ag_2C_2)(CF_3CO_2Ag)_5(15C5)_2(H_2O)]{\cdot}3H_2O$. (b) Triangulated dodecahedral silver(I) cage with two capping 12C4 ligands in $[Ag(12C4)_2]\{(Ag_2C_2)(AgCF_3CO_2)_8(CF_3CO_2)(12C4)_2(H_2O)_3\}{\cdot}H_2O$. (c) Sandwiched double cage in $[(Ag_2C_2)(AgCF_3CO_2)_5(benzo\text{-}15C5)(H_2O)_2]{\cdot}0.5H_2O$. (d) Triangulated dodecahedra (**A** and **C**) and bicapped trigonal antiprism (**B**) in $[Ag_4(18C6)_4(H_2O)_3]\{(Ag_2C_2)_3(AgCF_3CO_2)_{12}(CF_3CO_2)_4(H_2O)_{2.5}\}{\cdot}2.5H_2O$ [17].

meric structure containing a double cage fundamental unit. The double cage can be viewed as two monocapped trigonal prisms sharing an edge. Atom Ag4 is coordinated by all five oxygen atoms of the benzo-15C5 ligand with bond lengths in the range 2.391–2.788 Å (Fig. 8c). The double cage is further stabilized by the silver–aromatic interaction in the η^2 mode. Each sandwiched double cage is linked to neighboring ones by $[Ag_2(CF_3CO_2)_2]$ bridges to form an infinite chain.

When 18C6 was employed in the reaction, **$[Ag_4(18C6)_4(H_2O)_3]\{(Ag_2C_2)_3(AgCF_3CO_2)_{12}(CF_3CO_2)_4(H_2O)_{2.5}\}\cdot 2.5H_2O$** was isolated, which contains four independent $[Ag(18C6)]^+$ cations and one $\{(Ag_2C_2)_3(AgCF_3CO_2)_{12}(CF_3CO_2)_4(H_2O)_{2.5}\}^{4-}$ anionic moiety in the asymmetric unit. The cationic part is composed of silver(I) atoms each coordinated by a η^4-18C6 ligand and an additional water ligand in three of the four cases. The $[Ag(18C6)]^+$ cations are packed in stacks to induce the formation of an anionic column, which is generated through edge-sharing of three different silver polyhedra (Fig. 8d): two silver cages (**A**) and (**C**) are each in the shape of a triangulated dodecahedron, and the third (cage **B**) is a bicapped trigonal antiprism.

3.6. Formation of mixed-valent silver(I,II) complexes induced by tetraza macrocycles

The unique capability of the macrocyclic nitrogen-donor ligand to generate and stabilize a higher oxidation state of silver was exploited. The introduction of 1,4,8,11-tetramethyl-1,4,8,11-tetraazacyclotetradecane (tmc) as a co-ligand then led to the isolation of two novel mixed-valent silver(I,II) complexes [18].

$[Ag^{II}(tmc)(BF_4)]\{(Ag_2C_2)(AgCF_3CO_2)_4(CF_3CO_2)(H_2O)\}\cdot H_2O$ was prepared by dissolving Ag_2C_2 in an aqueous solution of CF_3CO_2Ag and $AgBF_4$, to which tmc was then added. The addition of tmc led to disproportionation of silver(I) to give elemental silver and complexed silver(II), and the latter was stabilized by tmc to form $[Ag^{II}(tmc)]^{2+}$. Weak axial interactions of the d^9 silver(II) center with adjacent BF_4^- ligands serve to link the complexed Ag(II) cations into an infinite $[Ag^{II}(tmc)(BF_4)]^{+1}_{\infty}$ chain. Induced by the presence of such a cationic chain, a parallel polymeric anionic column is assembled from the Ag(I), C_2^{2-} and $CF_3CO_2^-$ species; the building block of the backbone is a triangulated dodecahedron (Fig. 9a).

$[Ag^{II}(tmc)][Ag^{II}(tmc)(H_2O)]_2\{(Ag_2C_2)(AgCF_3CO_2)_9(CF_3CO_2)_3(H_2O)_4\}_2$ was obtained by adding tmc ligand to a concentrated aqueous solution of CF_3CO_2Ag containing dissolved Ag_2C_2. The tmc ligand readily induces the disproportionation of Ag(I) to elemental silver and Ag(II). The overall charge balance with respect to the silver(II) complex cations is provided by a silver(I) cluster dimer $[Ag_{11}^{I}(C_2)(CF_3CO_2)_{12}(H_2O)_4]_2^{6-}$. A basic polyhedral unit of this cluster can be described as a bicapped trigonal prism with one additional silver (Ag9) atom attached to one edge. There are two silver(I) atoms (Ag10 and Ag11) linked to this $[C_2@Ag_8]Ag$ system via carboxylate groups of the $CF_3CO_2^-$ ligands. A pair of water ligands of type $O1_W$ bridge two silver(I) atoms of type Ag_{10} to generate a centrosymmetric cluster dimer. In the absence of BF_4^- ions, the Ag(II) cations do not line up in a 1D array, and instead a dimeric supermolecular Ag(I) cluster anion is generated (Fig. 9b).

3.7. Quaternary ammonium cation-induced construction of high-nuclearity silver(I) complexes

Exploration of structural diversity by incorporating hydrophobic organic cations into the Ag_2C_2-containing system was carried out. The employment of quaternary ammonium cations favors the formation of anionic silver aggregates through the attainment of overall charge balance. Thus high-nuclearity silver(I) complexes can be harvested [19].

With tetraethylammonium tetrafluoroborate as a structure-inducing agent, **$[Et_4N]_6\{(Ag_2C_2)_2(AgCF_3CO_2)_8(CF_3CO_2)_3(H_2O)_2\}_2$** and **$[Et_4N]_3\{(Ag_2C_2)_2(AgCN)(AgCF_3CO_2)_{11}(CF_3CO_2)_3(H_2O)_6\}$** were prepared [19a]. **$[Et_4N]_6\{(Ag_2C_2)_2(AgCF_3CO_2)_8(CF_3CO_2)_3(H_2O)_2\}_2$** contains the discrete high-nuclearity cluster anion $[\{(Ag_2C_2)_2(AgCF_3CO_2)_8(CF_3CO_2)_3(H_2O)_2\}_2]^{6-}$, which is composed of two kinds of polyhedral units: a bicapped trigonal prism (cage **A**) and a triangulated dodecahedron (cage **B**) (Fig. 10a). Cages **A** and **B** share a triangular face to form a double cage, and two such double cages share an edge to generate a centrosymmetric

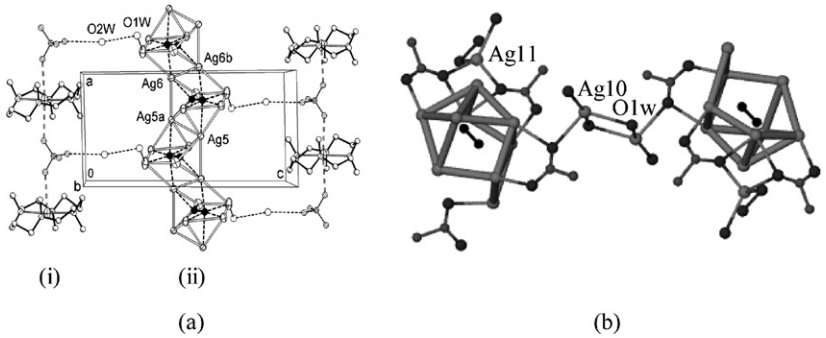

Fig. 9. (a) Crystal structure of $[Ag^{II}(tmc)(BF_4)]\{(Ag_2C_2)(AgCF_3CO_2)_4(CF_3CO_2)(H_2O)\}\cdot H_2O$: (i) column-like $[Ag^{II}(tmc)(BF_4)]^{+1}_{\infty}$ cationic column; (ii) polymeric $[Ag_6^{I}(C_2)(CF_3CO_2)_5(H_2O)]^{-1}_{\infty}$ zigzag chain generated from edge-sharing of silver(I) dodecahedra. (b) Perspective view of the structure of the dimeric supermolecular anion in $[Ag^{II}(tmc)][Ag^{II}(tmc)(H_2O)]_2\{(Ag_2C_2)(AgCF_3CO_2)_9(CF_3CO_2)_3(H_2O)_4\}_2$ [18].

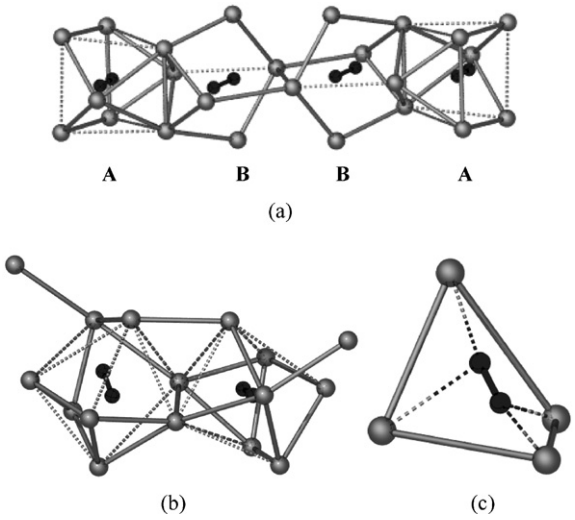

Fig. 10. (a) Centrosymmetric quadruple cage comprising 24 silver(I) atoms and four entrapped C_2^{2-} in $[Et_4N]_6\{(Ag_2C_2)_2(AgCF_3CO_2)_8(CF_3CO_2)_3(H_2O)_2\}_2$ [19a]. (b and c) Structure fragments of $(C_2)_2@Ag_{14}$, $[Ag_4CN]$ in $[Et_4N]_3\{(Ag_2C_2)_2(AgCN)(AgCF_3CO_2)_{11}(CF_3CO_2)_3(H_2O)_6\}$ [19a].

quadruple cage comprising 24 silver(I) atoms and 4 encapsulated acetylenediides. This discrete anionic cluster exhibits pseudo-symmetry *m*.

The core of **$[Et_4N]_3\{(Ag_2C_2)_2(AgCN)(AgCF_3CO_2)_{11}(CF_3CO_2)_3(H_2O)_6\}$** is a silver(I) double cage of symmetry 2, one half of which takes the shape of a triangulated dodecahedron that encapsulates a C_2^{2-} dianion. Two such polyhedra share an edge to generate the double cage, together with an additional vertex-to-vertex connection. Two pendant silver(I) atoms are each attached to a vertex of the double cage, yielding the $[(C_2)_2@Ag_{14}]Ag_2$ unit (Fig. 10b). The distorted cyanide ion is located at a site of symmetry 2 in a novel distorted tetrahedral environment (Fig. 10c). The silver(I) double cages and tetrahedra link up alternately to generate an infinite anionic silver(I) column $[\{(Ag_2C_2)_2(AgCN)(AgCF_3CO_2)_{11}(CF_3CO_2)_3(H_2O)_6\}^{3-}]_\infty$.

Further study using $(PhCH_2NMe_3)F$ as a structure-inducing agent led to the polymeric silver(I) complex **$\{[PhCH_2NMe_3](Ag_2C_2)(AgCF_3CO_2)_5(CF_3CO_2)\}_n$**, whose building unit is a square-antiprismatic silver(I) cluster. Silver polyhedra of this type share edges to generate an infinite chain (Fig. 11a) [19b]. The exterior η^3 π-donor behavior of the benzyltrimethylammonium ion attached to the silver(I) column observed here was found for the first time (Fig. 11b).

When benzyltrimethylammonium was introduced into the $Ag_2C_2/AgCF_3CO_2/AgNO_3$ system, **$[PhCH_2NMe_3]_4\{(Ag_2C_2)_2(AgCF_3CO_2)_{13}(CF_3CO_2)_3(NO_3)(H_2O)_4\}$** containing an anionic silver(I) column constructed with three kinds of anions was isolated [19c]. The basic building unit is an asymmetric silver double cage generated from the edge-sharing of a triangulated dodecahedron and a monocapped square antiprism (Fig. 12a). The nitrate ion functions as a μ_5-*O*,*O*,*O*′,*O*′,*O*″-bridge to link such double cages and two additional silver(I) atoms to generate an infinite columnar structure $[\{(Ag_2C_2)_2(AgCF_3CO_2)_{13}(CF_3CO_2)_3(NO_3)(H_2O)_4\}^{4-}]_\infty$ (Fig. 12b). This μ_5-ligation mode of the nitrate ion is unprecedented.

4. Betaine-induced assembly of neutral infinite columns and chains of linked silver(I) polyhedra with embedded acetylenediide dianion

Owing to their permanent bipolarity and overall charge neutrality, betaine ($Me_3N^+CH_2COO^-$, IUPAC name trimethylammonioacetate) and its derivatives (considered as carboxylate-type ligands) have distinct advantages over most carboxylates in the study of coordination polymers: (1) synthetic access to water-

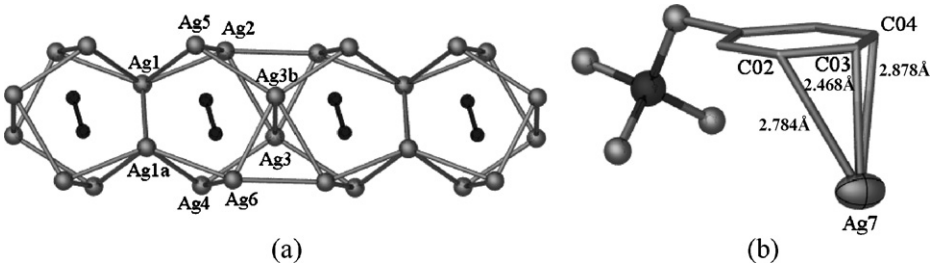

Fig. 11. (a) Square-antiprismatic silver(I) cages sharing edges of type Ag1···Ag1a and Ag3···Ag3b alternately to generate an infinite chain in $\{[PhCH_2NMe_3](Ag_2C_2)(AgCF_3CO_2)_5(CF_3CO_2)\}_n$. (b) η^3-Coordination of the phenyl group of the benzyltrimethylammonium ion to silver(I) [19b].

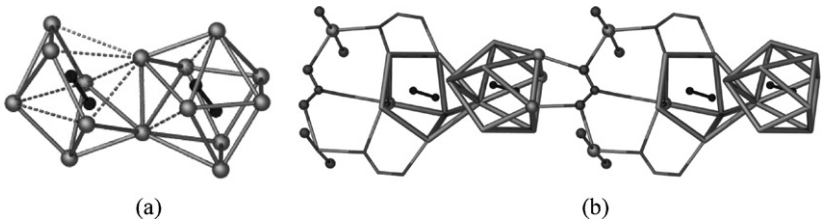

Fig. 12. (a) Asymmetric double cage unit $(C_2)_2@Ag_{15}$ composed of a triangulated dodecahedron and a monocapped square antiprism in $[PhCH_2NMe_3]_4\{(Ag_2C_2)_2(AgCF_3CO_2)_{13}(CF_3CO_2)_3(NO_3)(H_2O)_4\}$. (b) A portion of the silver(I) column constructed from $(C_2)_2@Ag_{15}$ polyhedra connected by μ_5-nitrate and trifluoroacetate bridges in $[PhCH_2NMe_3]_4\{(Ag_2C_2)_2(AgCF_3CO_2)_{13}(CF_3CO_2)_3(NO_3)(H_2O)_4\}$ [19c].

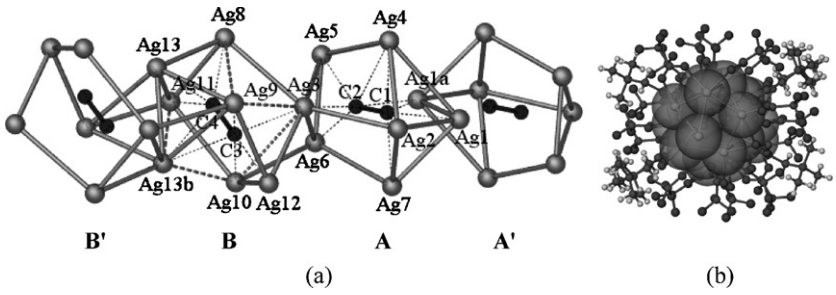

Fig. 13. (a) The infinite chain in $[(Ag_2C_2)_2(AgCF_3CO_2)_9(Me_3N^+CH_2COO^-)_3]$. (b) Perspective view along the *a* direction showing a hydrophobic sheath surrounding the silver(I) column with enclosed acetylenediide in $[(Ag_2C_2)_2(AgCF_3CO_2)_9(Me_3N^+CH_2COO^-)_3]$ [20].

soluble metal carboxylates; (2) generation of new structural varieties, such as complexes with metal centers bearing additional anionic ligands, and those with variable metal to carboxylate molar ratios; (3) easy modification of ligand properties by varying the substituents on the quaternary nitrogen atom or the backbone between the two polar terminals. The incorporation of betaine and its derivatives as zwitterionic ligands into the Ag_2C_2-containing system led to a series of new double salts of silver(I) acetylenediide bearing interesting structural motifs [20].

$[(Ag_2C_2)_2(AgCF_3CO_2)_9(Me_3N^+CH_2COO^-)_3]$ is composed of two kinds of silver(I) cages: a triangulated dodecahedron (cage **A**) and a bicapped trigonal prism (cage **B**) each encapsulating an acetylenediide dianion. A linear array of double cages **AA′** and **B′B** share vertices of type Ag3 with additional Ag···Ag contacts to generate an infinite silver(I) column **B′BAA′B′BAA′**··· (Fig. 13a). The trifluoroacetate and trimethylammonioacetate ligands function as μ_2- or μ_3-bridges across the Ag···Ag edges of the silver(I) column to form a hydrophobic sheath around it (Fig. 13b).

In the crystal structure of **$[(Ag_2C_2)_2(AgCF_3CO_2)_{10}(Me_3N^+CH_2CH_2COO^-)_3]\cdot H_2O$**, the building unit is a double cage generated from edge-sharing of a square-antiprism (cage **A**) and a distorted bicapped trigonal prism (cage **B**). Cage **A** and cage **B** share a triangular face to form a double cage (Fig. 14a). Double cages of this type are further fused together to form a helical column. This provides the first example of a helical silver(I) column with enclosed acetylenediide dianion. As found in $[(Ag_2C_2)_2(AgCF_3CO_2)_9(Me_3N^+CH_2COO^-)_3]$, this column is surrounded by a hydrophobic sheath composed of trifluoroacetate and trimethylammoniopropionate ligands (Fig. 14b).

The basic building block in **$[(Ag_2C_2)(AgCF_3CO_2)_7(Et_3N^+CH_2COO^-)_2(H_2O)]$** is a distorted monocapped cube. One of the seven independent trifluoroacetate groups and two triethylammonioacetate ligands act as μ_3-bridges across adjacent single cages to form a bead-like infinite chain (Fig. 15a).

In **$[(Ag_2C_2)(AgC_2F_5CO_2)_7(Me_3N^+CH_2COO^-)_3(H_2O)]$**, the core is a distorted monocapped square prism. The trimethylammonioacetate ligands in both μ_4-*O*,*O*,*O*′,*O*′ and μ_3-*O*,*O*,*O*′ modes, together with the μ_3-*O*,*O*,*O*′ trifluoroacetate ligands, link the $C_2@Ag_9$ motifs into a beaded chain (Fig. 15b). The replacement of trifluoroacetate ligands in $[(Ag_2C_2)_2(AgCF_3CO_2)_9(Me_3N^+CH_2COO^-)_3]$ with pfp ligands to give $[(Ag_2C_2)(AgC_2F_5CO_2)_7(Me_3N^+\ CH_2COO^-)_3(H_2O)]$ and the modification of the reaction conditions led to conversion of the

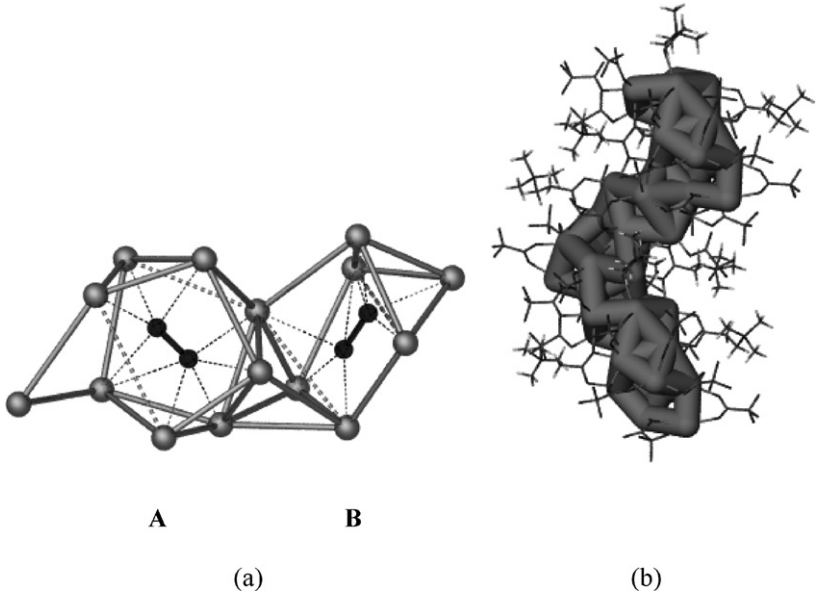

Fig. 14. (a) Double cage in $[(Ag_2C_2)_2(AgCF_3CO_2)_{10}(Me_3N^+CH_2CH_2COO^-)_3]\cdot H_2O$ arising from the fusion of a square-antiprism with a distorted bicapped trigonal prism. (b) Perspective view of the infinite silver(I) column with C_2^{2-} species embedded in its inner core and an exterior coat comprising anionic and zwitterionic carboxylates in $[(Ag_2C_2)_2(AgCF_3CO_2)_{10}(Me_3N^+CH_2CH_2COO^-)_3]\cdot H_2O$ [20].

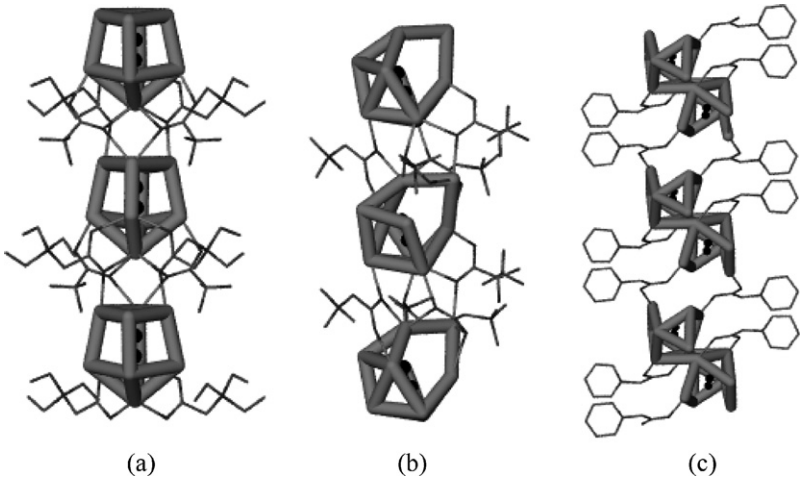

Fig. 15. (a) Perspective view of silver(I) bead-chain constructed from $C_2@Ag_9$ polyhedra connected by $Et_3N^+CH_2COO^-$ and trifluoroacetate bridges in $[(Ag_2C_2)(AgCF_3CO_2)_7(Et_3N^+CH_2COO^-)_2(H_2O)]$. (b) Portion of silver(I) chain generated from the linkage of discrete silver(I) cages via μ_3-*O*,*O*,*O*′ trifluoroacetate and $Me_3N^+CH_2COO^-$ ligands acting in μ_4-*O*,*O*,*O*′,*O*′ and μ_3-*O*,*O*,*O*′ coordination modes in $[(Ag_2C_2)(AgC_2F_5CO_2)_7(Me_3N^+CH_2COO^-)_3(H_2O)]$. (c) 1D chain-like structure of $[(Ag_2C_2)(AgC_2F_5CO_2)_6(C_5H_5N^+ CH_2COO^-)_2]$ generated from silver(I) cages linked by $C_5H_5N^+CH_2COO^-$ ligands [20].

fused silver column to a beaded chain of connected single cages. A plausible explanation is that the employment of the bulkier pfp ligands prohibited the fusion of silver cages.

The basic building unit in **$[(Ag_2C_2)(AgC_2F_5CO_2)_6(C_5H_5N^+CH_2COO^-)_2]$** is a centrosymmetric double cage composed of 16 silver(I) atoms, with each component single cage encapsulating an acetylenediide dianion. Each single cage is in the shape of an irregular monocapped trigonal prism with one additional atom. The μ_2-*O*,*O*′ coordination mode of pyridinioacetate links adjacent double cages to form an infinite chain (Fig. 15c).

$[(Ag_2C_2)(AgCF_3CO_2)_6(C_5H_5N^+CH_2COO^-)_2(H_2O)]\cdot H_2O$ has a 2D architecture. The basic building block is a centrosymmetric double cage with one embedded C_2^{2-} dianion in each triangulated dodecahedral single cage (Fig. 16a). The μ_2-*O*,*O*′ mode of pyridinioacetate ligands connect the double cages into an infinite chain. An interesting feature in is that the water ligands serve as bridging groups within the chain. The 2D structure is consolidated by cross-linkage of the chains through $[Ag_2(CF_3CO_2)_2]$ bridging (Fig. 16b).

It is noteworthy that irregular or highly distorted silver(I) cages generally occur in all the above-mentioned betaine-containing complexes, which may be attributed to the competition of the zwitterionic carboxylate groups with the C_2^{2-} dianion and perfluoroalkylcarboxylates for coordination sites around the silver(I) atoms.

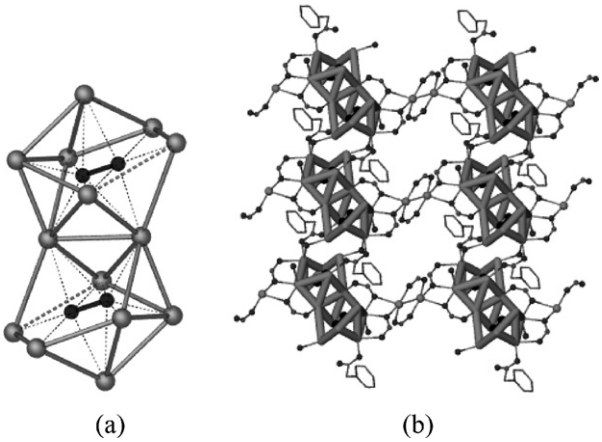

Fig. 16. (a) Centrosymmetric double cage in $[(Ag_2C_2)(AgCF_3CO_2)_6(C_5H_5N^+CH_2COO^-)_2(H_2O)]\cdot H_2O$, with each half taking the shape of a triangulated dodecahedron. (b) 2D structure formed from the linkage of silver(I) cages by $[Ag_2(CF_3CO_2)_2]$ units in $[(Ag_2C_2)(AgCF_3CO_2)_6(C_5H_5N^+CH_2COO^-)_2(H_2O)]\cdot H_2O$ [20].

5. Supramolecular assembly of silver(I) double/triple salts containing acetylenediide dianion

The foregoing work on the chemistry of Ag_2C_2 has demonstrated that $C_2@Ag_n$ polyhedra and fused double cages $(C_2)_2@Ag_{2n-m}$ (*n* vertices, *m* shared atoms) generally occur in its double, triple and quadruple salts due to the preference of C_2^{2-} for imprisonment inside a silver polyhedron. Our strategy in using $C_2@Ag_n$ polyhedra as building blocks for supramolecular assembly is to introduce bifunctional exodentate linkages between agglomerated components that are generated *in situ*. Such a synthetic approach has led to the isolation of a series of supramolecular complexes exhibiting distinctly different dimensionalities (discrete molecule, 1D, 2D and 3D networks).

All reactions were carried out using the hydrothermal method. Hydrothermal treatment is normally not advisable for a potentially explosive system containing Ag_2C_2; however, in the present instance, it did provide an effective route to obtain single crystals of good quality for structural characterization.

In a typical synthetic procedure, freshly prepared Ag_2C_2 was added to an aqueous solution containing one or more soluble silver(I) salts in a plastic beaker with stirring until saturation was attained. The excess amount of Ag_2C_2 was filtered off, and then an ancillary N/O-donor ligand was added.

The resulting suspension was placed in a 25 mL Teflon-lined stainless-steel reaction vessel and subjected to hydrothermal conditions at different temperatures ranging from 60 to 110 °C for 24–40 h, and subsequently cooled to room temperature at 6 °C/h.

5.1. With bifunctional exodentate nitrogen-donor ligands

The employment of bifunctional exodentate nitrogen-donor ligands into the reaction system results in a series of supramolecular complexes showing distinctly different crystal structures.

5.1.1. Discrete molecules

The addition of dabco (1,4-diazabicyclo[2.2.2.]octane) to a mixed aqueous solution of CF_3CO_2Ag and $AgBF_4$ containing dissolved Ag_2C_2 afforded a pale yellow precipitate, which was then manipulated under hydrothermal conditions to give **$[(Ag_2C_2)_2(AgCF_3CO_2)_{10}(CF_3CO_2)_4(dabcoH)_4(H_2O)_{1.5}]\cdot H_2O$** [21]. Its core is a $(C_2)_2@Ag_{14}$ double cage generated by edge-sharing of two distorted triangulated dodecahedra. This double cage exhibits pseudo-symmetry 2. The presence of trifluoroacetate, water and monoprotonated dabco ligands around the $(C_2)_2@Ag_{14}$ unit favors the isolation of a discrete molecule (Fig. 17a).

In the crystal structure of **$[Ag(bipyH)_2]_2\{(Ag_2C_2)_2(AgC_2F_5CO_2)_{12}(C_2F_5CO_2)_6\}\cdot 3H_2O$ (bipy = 4,4′-bipyridine)** [22], the building unit is a quasi-centrosymmetric double cage composed of 16 silver(I) atoms and 2 enclosed C_2^{2-} dianions, with each component single cage taking the shape of a monocapped square antiprism (Fig. 17b). The hydrophobic tails of pfp ligands obstruct further linkage between adjacent silver polyhedra, yielding a discrete supermolecule $[Ag_{16}(C_2)_2(C_2F_5CO_2)_{18}]^{6-}$. The four bipy ligands in the asymmetric unit are each protonated at one terminal to satisfy the charge balance. They are pairwise coordinated to the remaining silver(I) atoms, giving rise to two independent $[Ag(bipyH)_2]^{3+}$ cations, which promote the formation of the anionic Ag_{16} cluster.

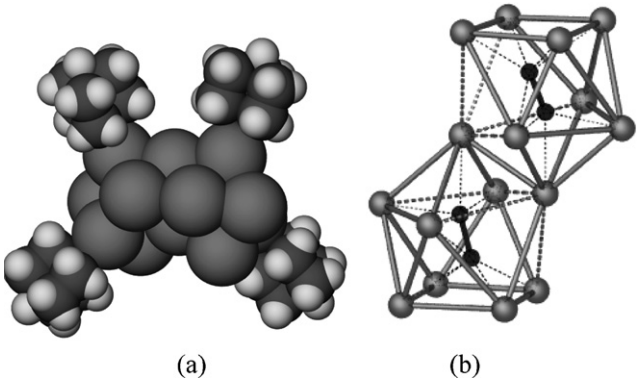

Fig. 17. (a) Space-filling drawing of the discrete supermolecule in $[(Ag_2C_2)_2(AgCF_3CO_2)_{10}(CF_3CO_2)_4(dabcoH)_4(H_2O)1.5]\cdot H_2O$, only the Ag atoms, C_2^{2-} species and dabcoH ligands are shown for clarity [21]. (b) Double cage unit $(C_2)_2@Ag_{16}$ in $[Ag(bipyH)_2]_2\{(Ag_2C_2)_2(AgC_2F_5CO_2)_{12}(C_2F_5CO_2)6\}\cdot 3H_2O$ generated from two monocapped square antiprisms sharing an edge [22].

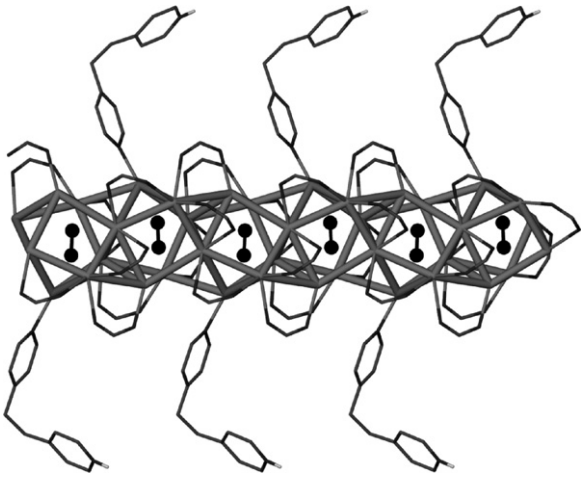

Fig. 18. Infinite branched-tree architecture in $[(Ag_2C_2)(AgCF_3CO_2)_4(CF_3CO_2)(bpaH)]_n$ [21].

5.1.2. 1D structures

$[(Ag_2C_2)(AgCF_3CO_2)_4(CF_3CO_2)(bpaH)]_n$ (bpa = 1,2-bis(4-pyridyl)ethane) has a branched-tree architecture, in which the basic building block is a distorted square antiprism [21]. Silver(I) cages of this type share edges and are consolidated by additional Ag···Ag interactions to generate an infinite chain-like silver(I) column that serves as the backbone of the herringbone array. One N terminal is protonated and the other is coordinated to a silver(I), and such ligation results in the attachment of cationic branches to the silver backbone (Fig. 18).

The virtually iso-structural complexes **$[(Ag_2C_2)(AgC_2F_5CO_2)_4(C_2F_5CO_2)(bppH)]_n$** and **$[(Ag_2C_2)(AgCF_3CO_2)_4(CF_3CO_2)(bppH)]_n$** (bpp = bis(4-pyridyl)propane) each has a branched-tree architecture [22]. The backbone is composed of fused monocapped trigonal prismatic $C_2@Ag_7$ silver(I) cages, with C_2^{2-} species embedded in its stem and an exterior coat composed of anionic perfluoroalkylcarboxyate and protonated bpp ligands.

5.1.3. 2D structures

In contrast to the synthesis of $[(Ag_2C_2)(AgCF_3CO_2)_4(CF_3CO_2)(bpaH)]_n$, minor variations in the synthetic conditions resulted in **$[(Ag_2C_2)(AgCF_3CO_2)_8(bpa)_4]_n$** exhibiting a 2D architecture [21]. The building unit in $[(Ag_2C_2)(AgCF_3CO_2)_8(bpa)_4]_n$ is a neutral decanuclear silver aggregate $[(Ag_2C_2)(AgCF_3CO_2)_8]$ of symmetry 2, which is composed of a distorted square-antiprismatic $C_2@Ag_8$ core, together with two additional silver(I) atoms and eight bridging $CF_3CO_2^-$ groups. The $[(Ag_2C_2)(AgCF_3CO_2)_8]$ moieties are connected by *anti*-type bpa ligands to form a chain, and such chains are further inter-linked by *gauche*-type bpa bridges to generate a layer structure (Fig. 19a).

$[(Ag_2C_2)(AgCF_3CO_2)_4(bpp)]$ has a bpp-bridged layer structure [22]. The basic building block is a $C_2@Ag_8$ single cage in the form of a distorted triangulated dodecahedron. Two single cages share an edge to form a centrosymmetric double cage, and such cages are further fused to form an infinite column via edge-sharing. The flexible bpp ligands, each with its $-CH_2CH_2CH_2-$

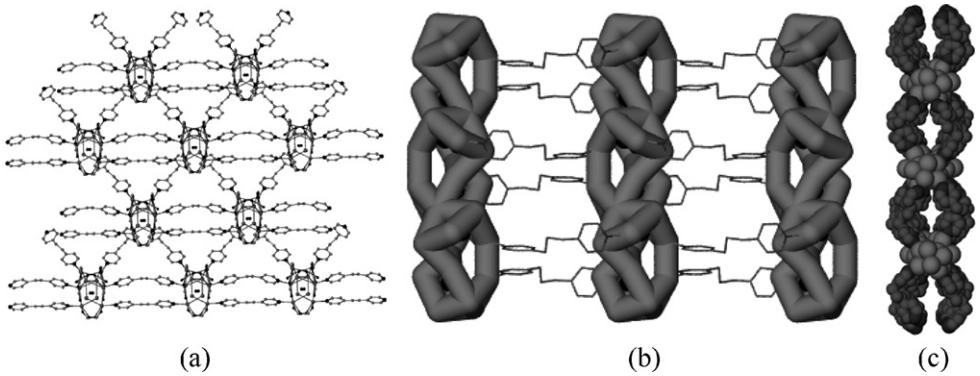

Fig. 19. (a) Layer structure in $[(Ag_2C_2)(AgCF_3CO_2)_8(bpa)_4]_n$ constructed from $[(Ag_2C_2)(AgCF_3CO_2)_8]$ moieties that are interconnected by both *anti*- and *gauch*-bpa ligands [21]. (b) 2D network of $[(Ag_2C_2)(AgCF_3CO_2)_4(bpp)]$ constructed from bpp-bridging of silver(I) columns [22]. (c) 2D structure in $[(Ag_2C_2)_4(AgCF_3CO_2)_{15}(bpp)_6]\cdot H_2O$ [22].

spacer adopting a TG conformation, further inter-link the infinite silver(I) columns to generate a 2D network (Fig. 19b).

Structural diversities have been observed in compounds: $[(Ag_2C_2)(AgCF_3CO_2)_4(bpp)]$ (2D), $[(Ag_2C_2)(AgC_2F_5CO_2)_4(C_2F_5CO_2)(bppH)]_n$ (1D), $[(Ag_2C_2)(AgCF_3CO_2)_4(CF_3CO_2)(bppH)]_n$ (1D) and **$[(Ag_2C_2)_4(AgCF_3CO_2)_{15}(bpp)_6]\cdot H_2O$** (2D) using the same ligand bpp via minor variations in the synthetic conditions. For $[(Ag_2C_2)_4(AgCF_3CO_2)_{15}(bpp)_6]\cdot H_2O$, the basic building block is an unusual example of a silver(I) column composed of four consecutive $C_2@Ag_n$ cages (one distorted monocapped trigonal prism, an irregular monocapped trigonal antiprism, and two distorted triangular dodecahedra) fused in a row. The bpp ligands taking the TG configuration connect the silver(I) columns into a 2D architecture (Fig. 19c) [22].

Another 2D network was found with bppz as the bridging ligands in **$[(Ag_2C_2)_2(AgCF_3CO_2)_{10}(bppz)_2(H_2O)]_n$** (bppz = 2,3-bis(2-pyridyl)pyrazine) [21]. The building unit is a silver(I) quadruple cage possessing $\bar{1}$ symmetry, which is composed of two kinds of single cages: a monocapped trigonal prism and a bicapped trigonal prism. These two single cages share an edge to form a double cage, and two such double cages related by an inversion center share an edge to generate the Ag_{24} building unit (Fig. 20a), which are further connected by bridging carboxylate groups to form a chain. The bppz ligand functions as an angular bridge to generate the 2D network (Fig. 20b).

5.1.4. 3D structures

$[(Ag_2C_2)(AgCF_3CO_2)_4(pyz)_2]_n$ (pyz = pyrazine) has a 3D framework composed of pyz-linked silver(I) columns [21]. The fundamental unit of the each column is a double cage made of two kinds of silver polyhedra: an irregular trigonal prism and a trigonal antiprism each enclosing an acetylenediide dianion. These cages are fused together to generate a silver(I) column, which are further cross-linked by pyz ligands to form a 3D framework (Fig. 21a).

At a reaction temperature of 60 °C, **$(Ag_2C_2)(AgCF_3CO_2)_6(3\text{-pyCN})_2$** with a 3D architecture was harvested [23]. The building unit is a double silver(I) cage with an inversion center. Each single cage containing an encapsulated C_2^{2-} species takes the form of a distorted triangulated dodecahedron. The double cages are further interconnected to generate a broken silver(I) column, which are inter-linked by 3-pyCN to form a 3D network (Fig. 21b).

$(Ag_2C_2)(AgCF_3CO_2)_4(4\text{-pyCN})_2$ was synthesized by the similar procedure as $(Ag_2C_2)(AgCF_3CO_2)_6(3\text{-pyCN})_2$ except that 4-cyanopyridine was used [23]. In the asymmetric unit, there are two similar $C_2@Ag_7$ cages and four independent 4-cyanopyridine ligands. Each $C_2@Ag_7$ cage takes the shape of a distorted pentagonal bipyramid. Single cages of each type are fused to adjacent cages through sharing of vertices and further vertex-to-vertex connections to form an infinite column. The silver(I) columns are further linked via 4-

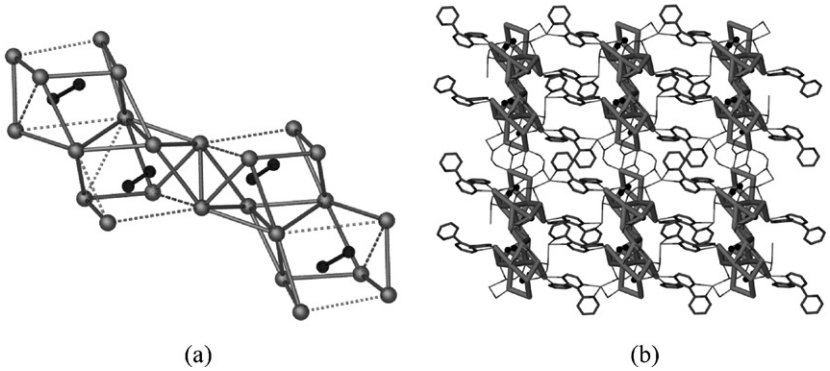

Fig. 20. (a) Centrosymmetric Ag_{24} quadruple cage units composed of edge-sharing of two types of cages in $[(Ag_2C_2)_2(AgCF_3CO_2)_{10}(bppz)_2(H_2O)]_n$. (b) 2D network of $[(Ag_2C_2)_2(AgCF_3CO_2)_{10}(bppz)_2(H_2O)]_n$ generated from quadruple cage units bridged by bppz ligands [21].

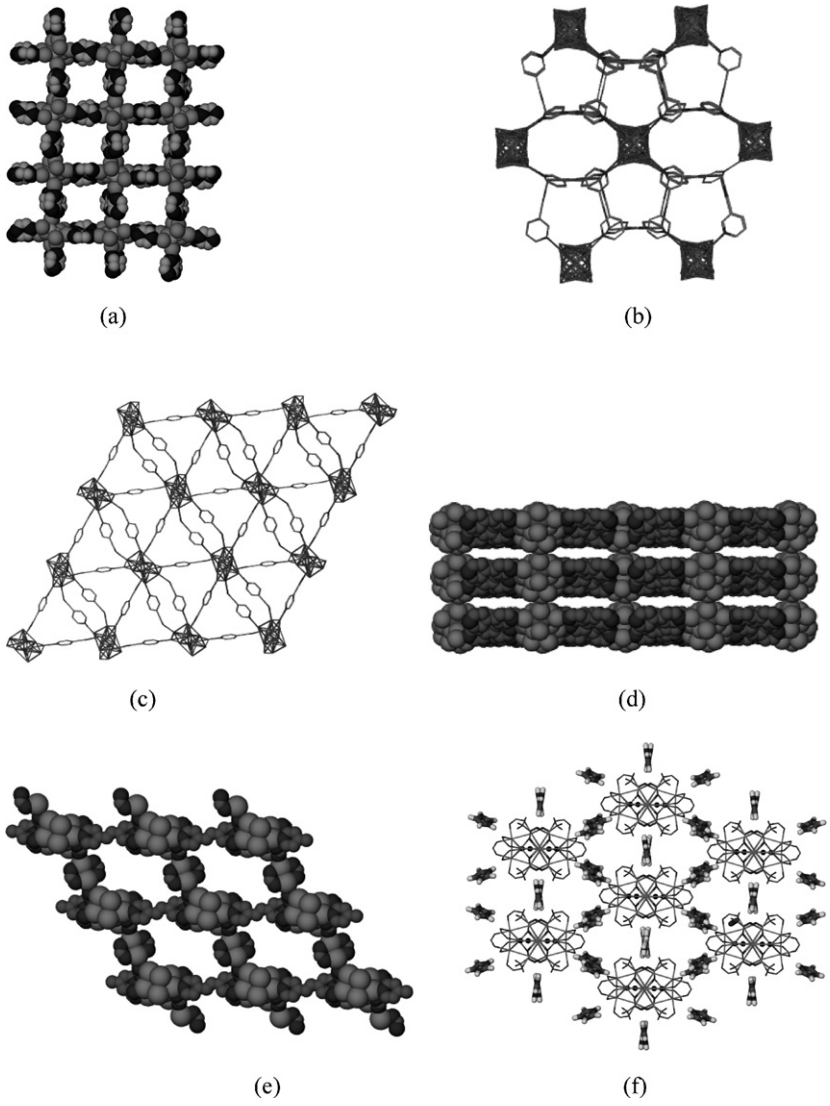

Fig. 21. (a) Space-filling drawing of the 3D framework of $[(Ag_2C_2)(AgCF_3CO_2)_4(pyz)_2]_n$ [21]. (b) The 3D network of $(Ag_2C_2)(AgCF_3CO_2)_6(3\text{-pyCN})_2$ [23]. (c) The (4,4) network bridged by 4-cyanopyridine ligands in $(Ag_2C_2)(AgCF_3CO_2)_4(4\text{-pyCN})_2$ [23]. (d) 3D architecture of $[(Ag_2C_2)_2(AgCF_3CO_2)_9(bipy)_4(H_2O)_3]$ generated from linkage of layers by argentophilic interactions [22]. (e) Space-filling diagram showing a cross-section of the 3D porous framework in $[(Ag_2C_2)_2(AgC_2F_5CO_2)_{10}(H_2O)_4(bpe)]\cdot H_2O$ [24]. (f) 3D architecture of $[imH]_3\{(Ag_2C_2)(AgCF_3CO_2)_6(CF_3CO_2)_3\}\cdot H_2O$ [24].

cyanopyridine ligands to form a doubly bridged (4,4) network (Fig. 21c).

The basic building block in **$[(Ag_2C_2)_2(AgCF_3CO_2)_9(bipy)_4(H_2O)_3]$** (bipy = 4,4′-bipyridine) is a double cage comprising 13 silver(I) atoms, with each component single cage encapsulating an acetylenediide dianion [22]. The double cage is generated from edge-sharing of a distorted pentagonal bipyramid and an irregular bicapped trigonal prism. Two such double cages share an edge to form a centrosymmetric Ag_{24} quadruple cage, whose remaining coordination sites are filled by the trifluoroacetate and water ligands. The $[(Ag_2C_2)_4(AgCF_3CO_2)_{16}(H_2O)_6]$ units are further connected by independent bipy ligands to form a layer. Argentophilic interactions between silver(I) atoms further connect the layers into a 3D architecture (Fig. 21d).

In the crystal structure of **$[(Ag_2C_2)_2(AgC_2F_5CO_2)_{10}(H_2O)_4(bpe)]\cdot H_2O$** (**bpe** = ***trans*-1,2-bis(4-pyridyl)ethylene**), the building block is a centrosymmetric $(C_2)_2@Ag_{14}$ double cage [24]. Each single cage is in the form of a distorted triangulated dodecahedron. The double cages are further fused together via edge-sharing to form an infinite silver(I) column. The 2D network is consolidated by cross-linkage of the columns through $[Ag_2(C_2F_5CO_2)_2]$. The rigid bpe ligands serve as connectors that further inter-link the layers into a porous 3D framework, with the hydrophobic pfp groups filling the channels (Fig. 21e).

The basic building block in **$[imH]_3\{(Ag_2C_2)(AgCF_3CO_2)_6(CF_3CO_2)_3\}\cdot H_2O$** (im = imidazole) is a $C_2@Ag_8$ single cage in the shape of a triangulated dodecahedron located on a two-fold axis [24]. Silver cages of this type are connected by μ_3-*O*,*O*,*O*′ trifluoroacetate ligands to form a zigzag anionic silver(I) column. All three independent imidazole moieties are protonated to provide the overall charge balance. Notably, the resulting $(imH)^+$ cations play a key role in the construction of the 3D architecture. The silver(I) columns are interconnected by

hydrogen bonding with the $(imH)^+$ cation serving as donors and *O*,*F* atoms of trifluoroacetate ligands as acceptors to form a 3D architecture (Fig. 21f).

5.2. With potential N,O-donor ligands

5.2.1. Discrete molecules

In the crystal structure of the first example of a 4-hydroxyquinoline (4-hq) metal complex, **[4-hq$_2$H]$_4${(Ag$_2$C$_2$)(AgCF$_3$CO$_2$)$_8$(CF$_3$CO$_2$)$_4$(4-hq)$_2$}·5H$_2$O** [25], the building unit is a novel $C_2@Ag_{10}$ silver cage in the shape of a bicapped square antiprism with symmetry 2. It is the largest silver(I) polyhedron found to date that encapsulates a C_2^{2-} dianion. Twelve $CF_3CO_2^-$ ligands in the μ-*O*,*O*′ mode and two 4-hq ligands in the μ-*O* coordination mode bridge the edges of $C_2@Ag_{10}$ to form an anionic $\{Ag_{10}(C_2)(CF_3CO_2)_{12}(4\text{-hq})_2\}^{4-}$ unit. To satisfy the overall charge balance, the uncoordinated 4-hq ligands are arranged in pairs whose O atoms are bridged by a proton. The resulting $(4\text{-hq}_2H)^+$ cations are attached to the Ag_{10} core via hydrogen bonds with their N–H groups serving as hydrogen bond donors and the trifluoroacetate ligands serving as acceptors (Fig. 22a).

The rhombohedral Ag_8 core in **Ag$_2$C$_2$·6AgCF$_3$CO$_2$·6(4-hq)** [25] is similar to that found in $Ag_2C_2{\cdot}6AgNO_3$ [10]. Likewise the encapsulated acetylenediide dianion is disordered about a crystallographic three-fold axis that bisects the C≡C bond and passes through two opposite corners of the Ag_8 rhombohedron. Apart from the μ-*O*,*O*′ trifluoroacetate ligands, there are six 4-hq ligands surrounding the polynuclear core, each bridging an edge in the μ-*O* mode. In contrast to $Ag_2C_2{\cdot}6AgNO_3$, in which the discrete cationic silver(I) polyhedra are inter-linked by nitrate ions to form a 3D network, $Ag_2C_2{\cdot}6AgCF_3CO_2{\cdot}6$ (4-hq) features a discrete $C_2@Ag_8$ cluster enveloped by bulky 4-hq and hydrophobic trifluoroacetate ligands, which prevent further linkage of adjacent silver(I) polyhedra (Fig. 22b).

In the crystal structure of **[(Ag$_2$C$_2$)(AgC$_2$F$_5$CO$_2$)$_6$(4-hq)$_3$(H$_2$O)]·H$_2$O** [25], the core is a centrosymmetric $(C_2)_2@Ag_{16}$ double cage with each component single cage taking the form of a distorted monocapped square antiprism. The $(C_2)_2@Ag_{16}$ double cage is surrounded by μ-*O*,*O*′ pfp, water and 4-hq ligands, which prevent further linkage between adjacent silver polyhedra, yielding a unique discrete supermolecule. The centroid–centroid distances between phenyl rings belonging to adjacent 4-hydroxyquinoline moieties are 3.708 and 3.725 Å, which fall within the normal range of π–π stacking interactions (Fig. 22c).

5.2.2. 2D structures

The basic building unit in **[4-hq·H$_3$O]$_2$[(Ag$_2$C$_2$)$_2$(AgC$_2$F$_5$CO$_2$)$_7$(C$_2$F$_5$CO$_2$)$_2$(H$_2$O)$_2$]·H$_2$O** is a $(C_2)_2@Ag_{12}$ double cage composed of two irregular monocapped trigonal antiprisms sharing an edge [25]. The double cages are fused together through sharing of vertices and additional Ag···Ag linkages to generate an infinite, sinuous anionic column. The O atoms of 4-hq and water molecule are bridged by a proton to give the cationic aggregate $(4\text{-hq}{\cdot}H_3O)^+$. The infinite silver(I) columns are further connected by hydrogen bonding with the $(4\text{-hq}{\cdot}H_3O)^+$ ions serving as donors and the F and O atoms of pfp as acceptors to form a hydrogen-bonded layer structure (Fig. 23a).

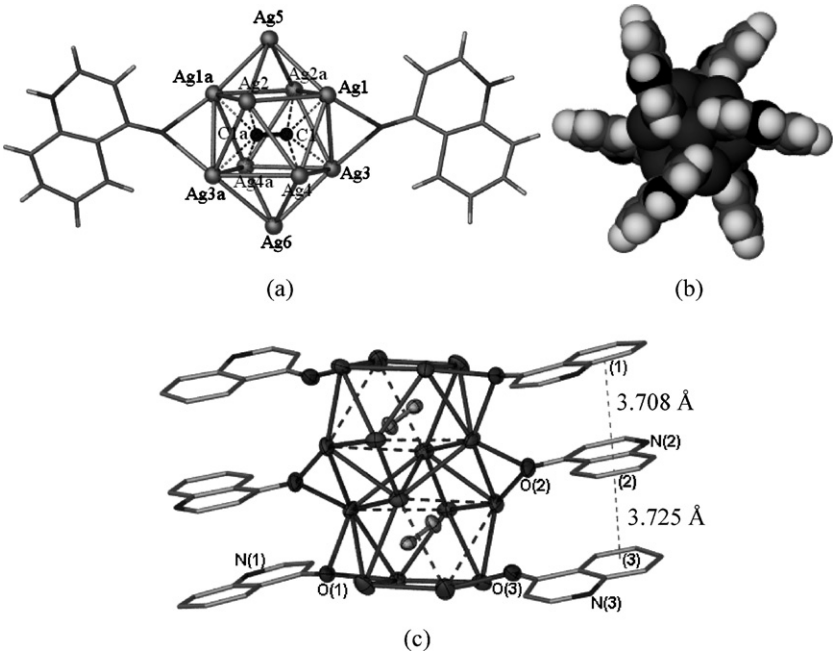

Fig. 22. (a) Bicapped square-antiprismatic $C_2@Ag_{10}$ core of the supramolecular anion $\{(Ag_2C_2)(AgCF_3CO_2)_8(CF_3CO_2)_4(4\text{-hq})_2\}^{4-}$ in $[4\text{-hq}_2H]_4[(Ag_2C_2)(AgCF_3CO_2)_8(CF_3CO_2)_4(4\text{-hq})_2]{\cdot}5H_2O$. This is the largest silver(I) polyhedron found to date that encapsulates a C_2^{2-} dianion [25]. (b) Space-filling drawing of the discrete supermolecule $Ag_2C_2{\cdot}6AgCF_3CO_2{\cdot}6(4\text{-hq})$ viewed along its three-fold symmetry axis. Trifluoroacetate ligands have been omitted for clarity [25]. (c) Structure of the centrosymmetric supermolecule in $[(Ag_2C_2)(AgC_2F_5CO_2)_6(4\text{-hq})_3(H_2O)]{\cdot}H_2O$ [25].

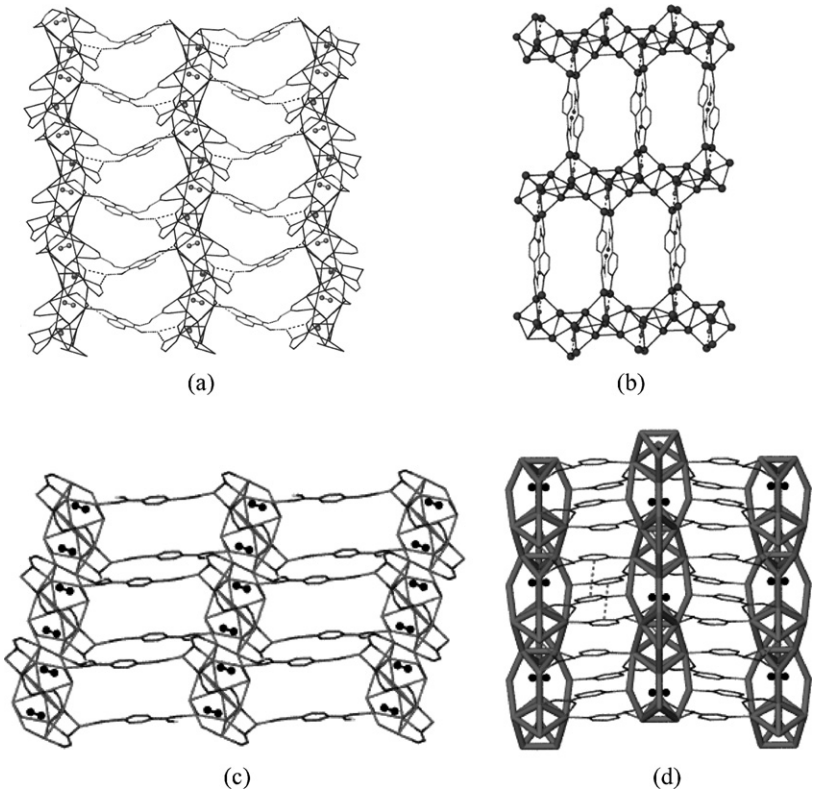

Fig. 23. (a) Schematic showing of the layer structure in $[4\text{-hq}\cdot H_3O]_2[(Ag_2C_2)_2(AgC_2F_5CO_2)_7(C_2F_5CO_2)_2(H_2O)_2]\cdot H_2O$ [25]. (b) Ball-and-stick drawing of the 2D structure of $[(Ag_2C_2)(AgCF_3CO_2)_4(4\text{-pyCONH}_2)(H_2O)]\cdot H_2O$ [23]. (c) 2D architecture of $[(Ag_2C_2)(AgC_2F_5CO_2)_5(4\text{-cbaH})(H_2O)_2]$ constructed from 4-cbaH-bridged silver(I) columns [24]. (d) The 2D structure formed from connection of silver(I) columns in $(Ag_2C_2)(AgCF_3CO_2)_2(3\text{-pyCOOAg})_2(3\text{-pyCOOH})_{1/2}$ [26].

The pyridine-4-carboxamide groups in **$[(Ag_2C_2)(AgCF_3CO_2)_4(4\text{-pyCONH}_2)(H_2O)]\cdot H_2O$** (4-pyCONH$_2$ = pyridine-4-carboxamide) originate from the hydrolysis of 4-cyanopyridine under hydrothermal condition [23]. Its basic building unit $C_2@Ag_8$ is in the shape of distorted triangulated dodecahedron. Such cage motifs share edges to generate a zigzag composite chain, which are further linked via pyridine-4-carboxamide to form a 2D network (Fig. 23b).

In **$[(Ag_2C_2)(AgC_2F_5CO_2)_5(4\text{-cbaH})(H_2O)_2]$** (4-cbaH = 4-cyanobenzoic acid) the core is a centrosymmetric $(C_2)_2@Ag_{14}$ double cage constructed from face-sharing of two $C_2@Ag_8$ single cages, each having the geometry of a distorted bicapped trigonal prism. Such double cages are fused together via edge-sharing to generate an infinite silver(I) column. Inter-linkage of silver(I) columns *via* neutral 4-cbaH generates a 2D network (Fig. 23c) [24].

In **$(Ag_2C_2)(AgCF_3CO_2)_2(3\text{-pyCOOAg})_2(3\text{-pyCOOH})_{1/2}$** (3-pyCOOH = nicotinic acid), the basic building unit is a $(C_2)_2@Ag_{14}$ double cage of symmetry *m*, with two component single cages each taking the shape of a triangulated dodecahedron [26]. The double cages are further fused together via edge-sharing to generate an infinite column. Of the three nicotinate fragments in the asymmetric unit, neutral 3-pyCOOH lies in the mirror plane and coordinates to one silver(I) atom, whereas the two anionic 3-pyCOO groups bind to the silver(I) atoms in the μ_3-*O*,*O*′,*N* mode to connect the columns into a 2D structure (Fig. 23d).

5.2.3. 3D structures

Similar to the case in $[(Ag_2C_2)(AgCF_3CO_2)_4(4\text{-pyCONH}_2)(H_2O)]\cdot H_2O$, ligand 3-cyanopyridine undergoes hydrolysis under hydrothermal conditions in the $AgCF_3CO_2/AgBF_4/Ag_2C_2$ reaction system to the form **$(Ag_2C_2)(AgCF_3CO_2)_8(3\text{-pyCONH}_2)_2(H_2O)_4$** [23]. The basic building unit is a square-antiprismatic $C_2@Ag_8$ silver cage of imposed C_2 symmetry. The cages are linked by μ_3-*O*,*O*,*O*′ trifluoroacetate ligands to generate a columnar structure. Another silver(I) atom in a trigonal planar environment is surrounded by the pyridyl nitrogen atom of 3-pyCONH$_2$ and two water ligands, thus serving as one branch of the architecture. It is noteworthy that hydrogen bonds with the amino group of 3-pyCONH$_2$ and water ligands serving as donors and the oxygen atoms of the trifluoroacetate group as acceptors further connect the columns into a 3D scaffold (Fig. 24a).

Structural analysis showed that **$(Ag_2C_2)(AgCF_3CO_2)_6(3\text{-pyCONH}_2)_4$** (3-pyCONH$_2$ = pyridine-3-carboxamide) has a 3D framework composed of $C_2@Ag_8$ cages inter-linked by pyridine-3-carboxamide ligands [23]. There are three similar independent silver cages in the asymmetric unit, each taking the shape of a distorted bicapped trigonal prism, which are inter-linked by 3-pyCONH$_2$ groups to form a 3D architecture.

The basic building block in **$[(Ag_2C_2)(AgCF_3CO_2)_2(4\text{-cbaAg})_3]$** is a centrosymmetric $(C_2)_2@Ag_{14}$ double cage [24]. Each component single cage takes the shape of a distorted bicapped trigonal prism. Such double cages are connected by

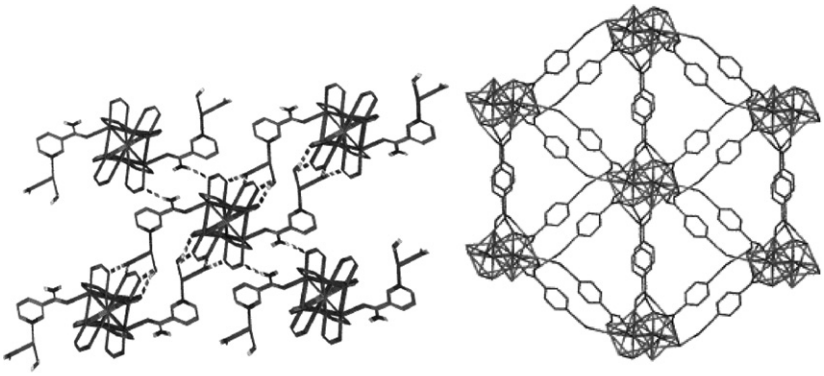

Fig. 24. (a) 3D architecture of $(Ag_2C_2)(AgCF_3CO_2)_8(3\text{-}pyCONH_2)_2(H_2O)_4$ resulting from the linkage of silver(I) columns *via* hydrogen bonds [23]. (b) Schematic showing the (3,6) network in $[(Ag_2C_2)(AgCF_3CO_2)_2(4\text{-}cbaAg)_3]$ [24].

argentophilic interactions to form an infinite column. The silver(I) columns are arranged in a hexagonal array, and each column is linked to an adjacent one by a pair of 4-cba ligands. Three neighboring silver columns encircle a triangular channel, and a cross-section of the 3D network has the (3,6) (or 3^6) topology (Fig. 24b).

The basic building block of triple salt **$(Ag_2C_2)(AgNO_3)_4(3\text{-}pyCO_2Ag)_2(3\text{-}pyCOOH)_2$** is a discrete $C_2@Ag_8$ cage in the shape of a bicapped trigonal prism of symmetry *m* [26]. The μ_3-*O*,*O*,*O* coordination mode of nitrate ligands link the $C_2@Ag_8$ cages into an infinite zigzag silver(I) chain. The composite chains are then linked by anionic nicotinate anions to form a 2D network. A 3D architecture is generated with neutral 3-pyCOOH groups connecting the 2D network (Fig. 25).

The basic building unit in **$\{(Ag_2C_2)(AgCF_3CO_2)_4(4\text{-}pyCOO)(H_2O)\}\cdot[4\text{-}pyCOOH_2]$** (4-pyCOOH = isonicotinic acid) is a centrosymmetric double cage composed of 12 silver(I) atoms, with each component cage encapsulating an acetylenediide dianion [26]. Each single cage is an irregular pentagonal bipyramid. Argentophilic interactions further connect the double cages into an infinite chain. The composite chains are linked via anionic 4-$pyCO_2$ groups to form a layer structure. The most intriguing features of $\{(Ag_2C_2)(AgCF_3CO_2)_4(4\text{-}pyCOO)(H_2O)\}\cdot[4\text{-}pyCOOH_2]$ arise from interactions at the supramolecular level. To satisfy the overall charge balance, the uncoordinated 4-pyCOOH is protonated at its nitrogen terminal to form $[4\text{-}pyCOOH_2]^+$. Such $[4\text{-}pyCOOH_2]^+$ cations function as pillars in connecting the layers, serving as hydrogen-bond donors with the trifluoroacetate O atoms and the coordinated 4-$pyCO_2$ ligands as acceptors, to yield a 3D architecture (Fig. 26).

In the crystal structure of **$(Ag_2C_2)(AgNO_3)_3(2\text{-}pyzCO_2Ag)_2$ ($2\text{-}pyzCO_2H$ = 2-pyrazinecarboxylic acid)**, the building unit is a $C_2@Ag_7$ single cage in the shape of a distorted monocapped trigonal prism [26]. The μ_3-*O*,*O*′,*O*″ and μ_4-*O*,*O*,*O*′,*O*″ coordination modes of nitrate ions connect the single $C_2@Ag_7$ cages into planar layers, which are further bridged by anionic 2-$pyzCO_2$ to form a 3D architecture (Fig. 27).

$[(Ag_2C_2)(AgCF_3CO_2)_4(2\text{-}pyzCO_2Ag)_2(H_2O)_2]\cdot H_2O$ has a 3D architecture, in which the basic building block is a $C_2@Ag_8$ cage in the shape of a triangulated dodecahedron [26]. One 2-$pyzCO_2$ and two trifluoroacetate ligands in the μ_3-*O*,*O*,*O*′ coordination modes link the $C_2@Ag_8$ cages to form an infinite chain. The pyrazine parts of this 2-$pyzCO_2$ further links the silver(I) chains into a layer. Another 2-$pyzCO_2$ ligand acting in the μ_5-*N*,*N*′,*O*,*O*,*O*′ mode further links the layers to generate the 3D architecture (Fig. 28).

6. Ligand-induced disruption of polyhedral $C_2@Ag_n$ cage assembly

6.1. With pyrazine-2-carboxamide

The previously reported structural motifs are all convex polyhedra with only one C_2^{2-} entrapped in each cage. Attempts to interfere with the assembly process to open the $C_2@Ag_n$

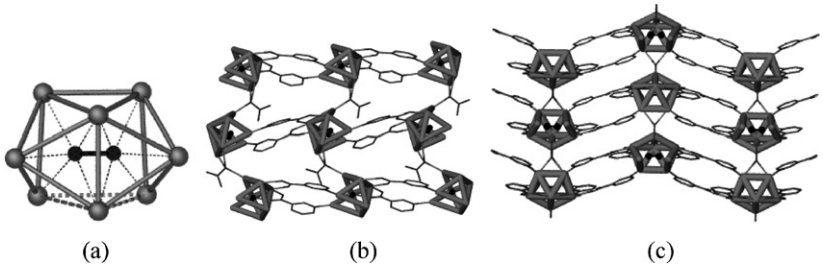

Fig. 25. (a) The basic building block of $(Ag_2C_2)(AgNO_3)_4(3\text{-}pyCO_2Ag)_2(3\text{-}pyCOOH)_2$ in the shape of bicapped trigonal prism of symmetry *m*. (b) The 2D network generated from linkage of silver(I) chains via anionic nicotinic ligands in $(Ag_2C_2)(AgNO_3)_4(3\text{-}pyCO_2Ag)_2(3\text{-}pyCOOH)_2$. (c) Ball-and-stick showing of the 3D architecture of $(Ag_2C_2)(AgNO_3)_4(3\text{-}pyCO_2Ag)_2(3\text{-}pyCOOH)_2$ [26].

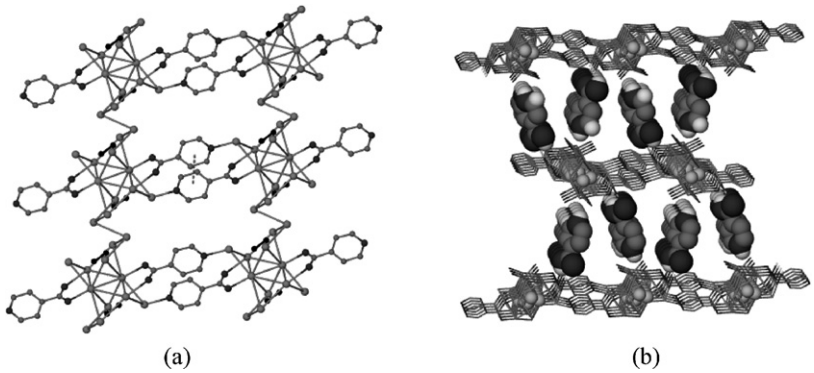

Fig. 26. (a) 2D network generated from linkage of composite silver(I) chains in $\{(Ag_2C_2)(AgCF_3CO_2)_4(4\text{-pyCOO})(H_2O)\}\cdot[4\text{-pyCOOH}_2]$. (b) The 3D architecture of $\{(Ag_2C_2)(AgCF_3CO_2)_4(4\text{-pyCOO})(H_2O)\}\cdot[4\text{-pyCOOH}_2]$, with $[4\text{-pyCOOH}_2]^+$ serving as hydrogen-bond connectors to adjacent layers [26].

cage or construct a large single cage for holding two or more C_2^{2-} species were carried out via the incorporation of the multidentate ligand pyzCONH$_2$ (pyrazine-2-carboxamide) into the reaction system. Pyrazine-2-carboxamide was selected as a structure-directing component in view of its very short spacer length and chelating capacity, and the introduction of the amide functionality could conceivably disrupt the assembly of $C_2@Ag_n$ via the formation of hydrogen bonds. Two new silver(I) complexes exhibiting novel $C_2@Ag_n$ motifs were obtained: **$[(Ag_2C_2)_2(AgCF_3CO_2)_8(2\text{-pyzCONH}_2)_3]$** and **$[(Ag_2C_2)_4(AgC_2F_5CO_2)_8(2\text{-pyzCOOAg})_4(2\text{-pyzCONH}_2)(H_2O)_2]$**.

Double salt $[(Ag_2C_2)_2(AgCF_3CO_2)_8(2\text{-pyzCONH}_2)_3]$ was prepared by dissolving Ag_2C_2 in an aqueous solution of CF_3CO_2Ag and $AgBF_4$ followed by the addition of pyrazine-2-carboxamide [27]. The resulting precipitate was then subjected to hydrothermal condition. In the crystal structure of $[(Ag_2C_2)_2(AgCF_3CO_2)_8(2\text{-pyzCONH}_2)_3]$, the basic structural unit comprises the fusion of a distorted triangulated dodecahedral Ag_8 cage containing an embedded C_2^{2-} dianion and an open fish-like $Ag_6(\mu_6\text{-}C_2)$ motif (Fig. 29).

In the $Ag_6(\mu_6\text{-}C_2)$ motif, atom C3 is embraced by four silver atoms in a butterfly arrangement and C4 bonds to two silver

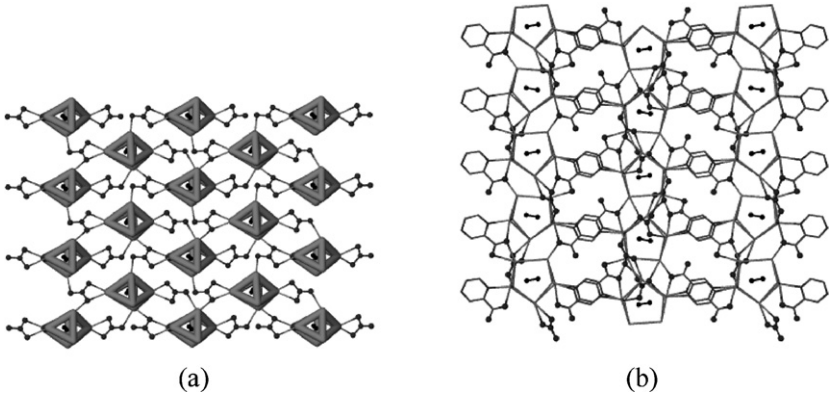

Fig. 27. (a) 2D structure formed from nitrate-connected $C_2@Ag_7$ cages in $(Ag_2C_2)(AgNO_3)_3(2\text{-pyzCO}_2Ag)_2$. (b) Ball-and-stick showing of the 3D architecture of $(Ag_2C_2)(AgNO_3)_3(2\text{-pyzCO}_2Ag)_2$ [26].

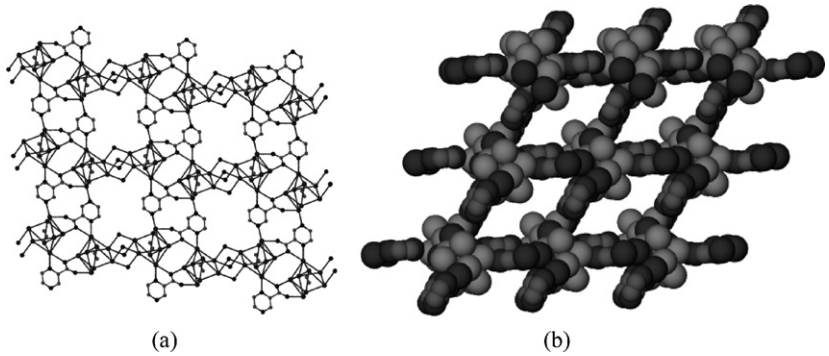

Fig. 28. (a) 2D plane generated from linkage of $C_2@Ag_8$ single cages in $[(Ag_2C_2)(AgCF_3CO_2)_4(2\text{-pyzCO}_2Ag)_2(H_2O)_2]\cdot H_2O$. (b) Space-filling drawing of the 3D architecture of $[(Ag_2C_2)(AgCF_3CO_2)_4(2\text{-pyzCO}_2Ag)_2(H_2O)_2]\cdot H_2O$ [26].

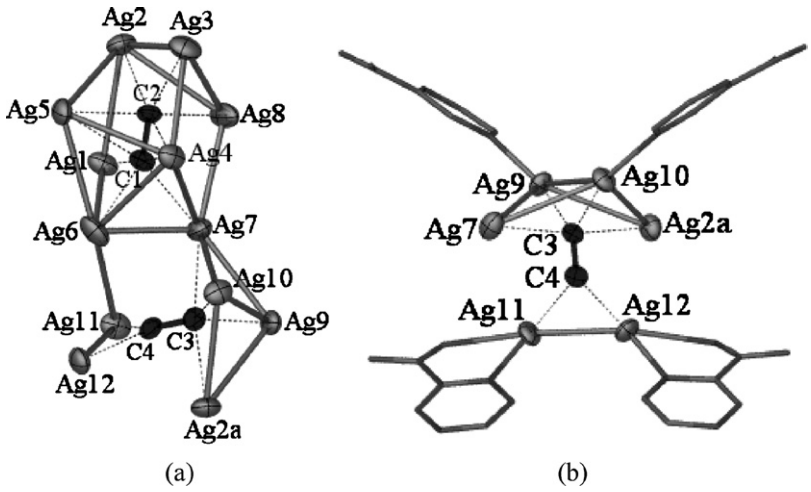

Fig. 29. (a) Basic building unit in $Ag_{12}(C_2)_2(CF_3CO_2)_8(2\text{-pyzCONH}_2)_3$. (b) Open fish-like $Ag_6(\mu_6\text{-}C_2)$ motif coordinated by four pyrazine-2-carboxamide ligands in $Ag_{12}(C_2)_2(CF_3CO_2)_8(2\text{-pyzCONH}_2)_3$ [27].

atoms. The existence of such an open motif can be rationalized by the fact that it is stabilized by four surrounding pyrazine-2-carboxamide ligands, so that steric overcrowding obstructs the aggregation of silver(I) into a closed cage. The $Ag_6(\mu_6\text{-}C_2)$ motif may be visualized as an intermediate moiety that is prevented by the surrounding pyrazine-2-carboxamide ligands from developing into a polyhedral $C_2@Ag_n$ aggregate during crystal growth.

In the synthesis of triple salt $[(Ag_2C_2)_4(AgC_2F_5CO_2)_8(2\text{-pyzCOOAg})_4(2\text{-pyzCONH}_2)(H_2O)_2]$, a major portion of pyrazine-2-carboxamide underwent hydrolysis to pyrazine-2-carboxylate, resulting in the first example of their co-existence as mixed ligands in a metal complex [27].

The basic building block in $[(Ag_2C_2)_4(AgC_2F_5CO_2)_8(2\text{-pyzCOOAg})_4(2\text{-pyzCONH}_2)(H_2O)_2]$ is an aggregate composed of three polyhedral units: an unprecedented partially opened cage $(C_2)_2@Ag_{13}$ (cage **A**) and two similar distorted $C_2@Ag_6$ trigonal prisms (cages **B** and **C**) (Fig. 30).

A pair of C_2^{2-} dianions is completely encapsulated in cage **A**. For simplicity, this Ag_{13} single cage can be visualized as composed of two distorted cubes sharing a common face, with cleavage of four of the edges and capping of the lateral (Ag5Ag9Ag12Ag8) face by Ag13 lying 1.9 Å above it. The two embedded C_2^{2-} dianions retain their triple-bond characters with similar C–C bond lengths of 1.18(2) Å and exhibit multiple σ and π interactions with the cage silver(I) atoms with Ag–C bond distances in the range 2.14(2)–2.55(2) Å. The Ag···Ag distances lie in the range 2.821(2)–3.237(2) Å. The interatomic distances of Ag6···Ag5 (4.181 Å), Ag5···Ag8 (3.820 Å), Ag7···Ag8 (3.692 Å), and Ag8···Ag12 (3.738 Å) are too long for significant argentophilic interaction. Cage **A** thus provides the first example of two C_2^{2-} dianions trapped inside a single cage.

Cages **B** and **C** each takes the shape of a distorted trigonal prism with one encapsulated C_2^{2-} dianion. The trapped C_2^{2-} species retains its triple-bond character (C5–C6 1.22(2) for cage **B** and C7–C8 1.20(2) Å for cage **C**) while having multiple interactions with its adjacent silver atoms.

6.2. With ligands of the pyridine-N-oxide type

Further studies on structural diversity by incorporating other ancillary ligands that could affect the formation of regular $C_2@Ag_n$ aggregates were carried out. Ligands of the pyridine-*N*-oxide (pyO) class for the construction of new $C_2@Ag_n$ motifs were incorporated. The pyO-type ligands differ from pyridine-type ligands in several aspects: (a) oxygen is a harder donor than nitrogen; (b) the coordination preference between pyO and pyridine is quite different, as each oxygen site in pyO may bridge two or more metal centers while the nitrogen donor in pyridine is always coordinated to one metal center; (c) the pyO-type is

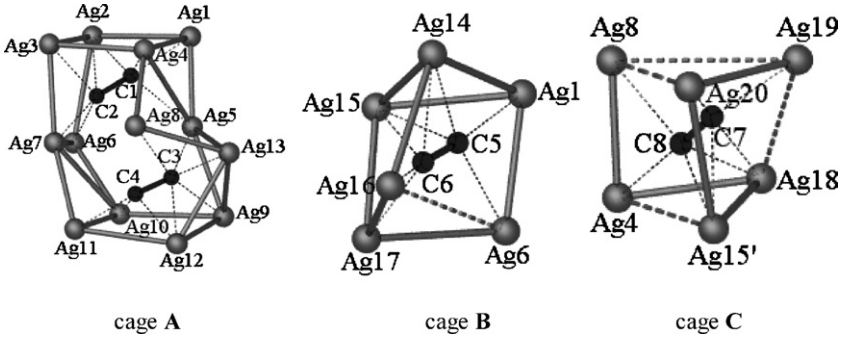

Fig. 30. Three different kinds of silver polyhedra in the crystal structure of $Ag_{20}(C_2)_4(C_2F_5CO_2)_8(2\text{-pyzCOO})_4(2\text{-pyzCONH}_2)(H_2O)_2$ [27].

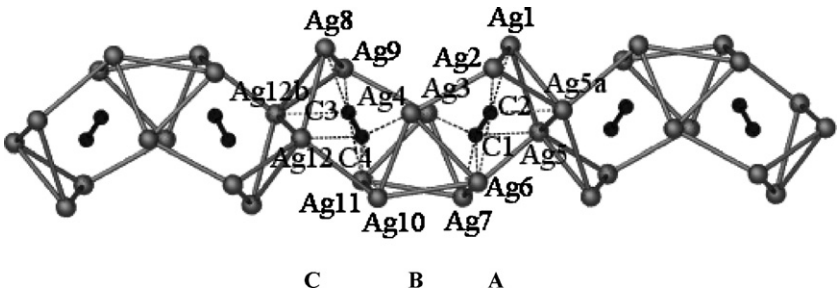

Fig. 31. Portion of zigzag silver(I) column in $(Ag_2C_2)_2(AgCF_3CO_2)_8(pyO)_{3.5}$ generated from fusion of $(C_2)_2@Ag_{14}$ aggregates, each constructed from polyhedra labeled A, B and C [28].

a longer spacer, which allows for the formation of more porous structures. Proceeding on the premise that the highly polar pyO group can compete with the acetylenediide for coordination to silver, a series of pyO-type ligands were employed for the construction of such cage motifs [28].

$(Ag_2C_2)_2(AgCF_3CO_2)_8(pyO)_{3.5}$ was prepared by dissolving Ag_2C_2 in an aqueous solution of CF_3CO_2Ag and $AgBF_4$ followed by the addition of nicotinic acid *N*-oxide; the afforded precipitate was then treated under hydrothermal condition. The *in situ* generation of pyO from nicotinic acid *N*-oxide takes place at a low reaction temperature of 110 °C.

In the crystal structure of $(Ag_2C_2)_2(AgCF_3CO_2)_8(pyO)_{3.5}$, the building block is a $(C_2)_2@Ag_{14}$ aggregate composed of 14 silver(I) atoms and a pair of encapsulated acetylenediides. The Ag_{14} aggregate can be visualized as constructed from two quite distorted square antiprisms (part **A** and part **C**) and a distorted trigonal antiprism (part **B**), with cleavage of five of the edges (Fig. 31).

Parts **A**, **B** and **C** are fused via sharing of vertices to form an irregular Ag_{14} aggregate, which has a pseudo-two-fold axis passing through the mid-point of the Ag3···Ag4 link and the center of the non-planar (Ag6Ag7Ag11Ag10) tetragon. The Ag···Ag distances lie in the range 2.805(2)–3.222(2) Å. The interatomic distances of Ag3···Ag4 (3.772 Å), Ag1···Ag3 (3.559 Å), Ag5a···Ag6 (3.536 Å), Ag4···Ag8 (3.546 Å), and Ag11···Ag12a (3.483 Å) are too long for significant argentophilic interaction (over twice the van der Waals radius of silver) and thus result in the new cage type. In contrast to the case in $Ag_{20}(C_2)_4(C_2F_5CO_2)_8(2\text{-pyzCOO})_4(2\text{-pyzCONH}_2)(H_2O)_2$ in which two C_2^{2-} dianions are trapped inside a Ag_{13} single cage, the $(C_2)_2@Ag_{14}$ aggregate found here is differently assembled.

In the crystal structure of **$(Ag_2C_2)(AgCF_3CO_2)_4(bppO_2)$** ($bppO_2$ = 1,3-bis(4-pyridyl)propane-*N*,*N*′-dioxide), the core is a centrosymmetric $(C_2)_2@Ag_{12}$ double cage. Each component $C_2@Ag_7$ single cage can be described as a distorted triangulated dodecahedron with removal of one vertex, and thus the C_2^{2-} dianion is enclosed in the partially open Ag_7 cage (Fig. 32a).

In the crystal structure of **$[(Ag_2C_2)(AgCF_3SO_3)_3(bppO_2Ag)_2(H_2O)_2]\cdot 2CF_3SO_3$**, the core is a $C_2@Ag_7$ single cage in the form of a slightly distorted monocapped

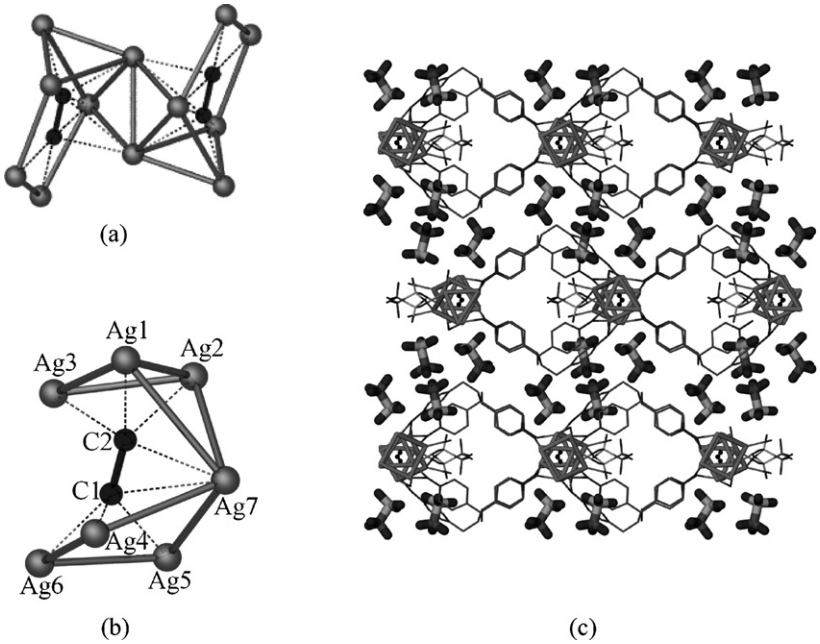

Fig. 32. (a) Centrosymmetric $(C_2)_2@Ag_{12}$ double cage in $(Ag_2C_2)(AgCF_3CO_2)_4(bppO_2)$. (b) Deformed $C_2@Ag_7$ single cage in $[(Ag_2C_2)(AgCF_3SO_3)_3(bppO_2Ag)_2(H_2O)_2]\cdot 2CF_3SO_3$. (b) Layer-type structure of $[(Ag_2C_2)(AgCF_3SO_3)_3(bppO_2Ag)_2(H_2O)_2]\cdot 2CF_3SO_3$ constructed from triflate and $bppO_2$-linking $C_2@Ag_7$ cages, with free triflate moieties accommodated between the host layers [28].

trigonal prism with cleavage of four edges (Fig. 32b). The two independent $bppO_2$ ligands exhibit different TG and GG conformations. Their respective μ_3-*O*,*O*,*O*′ and μ_4-*O*,*O*,*O*′,*O*′ coordination modes, together with one μ_2-*O*,*O*′ triflate and the water ligand, connect the $C_2@Ag_7$ cages into an infinite chain. The composite chains are then further inter-linked by $bppO_2$ to form a cationic layer structure. The free triflate moieties are accommodated between the cationic host layers, thus forming an inclusion complex, which represents the first example of a layer-type cationic host structure containing $C_2@Ag_n$ that features the inclusion of anions (Fig. 32c).

7. Summary

The formation of the $C_2@Ag_n$ ($n = 6$–10) polyhedra is a facile process that can be influenced by many factors. In our systematic studies, to satisfy the charge balance and coordination environment of silver(I), co-existing anions such as fluoride, perchlorate, nitrate, tetrafluoroborate and triflate, as well as perfluoro-substituted alkylcarboxylates and dicaboxylates, were introduced into the Ag_2C_2-containing reaction systems to obtain a wide variety of double, triple and quadruple salts. Subsequently, the influence of neutral ancillary ligands such as aliphatic nitriles and crown ethers was explored. Employment of the tetraza macrocycle ligand 1,4,8,11-tetramethyl-1,4,8,11-tetraazacyclotetradecane then led to the isolation of mixed-valent silver(I,II) complexes. Furthermore, the role of quaternary ammonium cations (Et_4N^+, Me_3BzN^+) in the generation of polynuclear silver(I) aggregates containing C_2^{2-} was investigated. Incorporation of betaine and its derivatives into the Ag_2C_2-containing system was explored on the premise that this type of zwitterionic ligand could compete with acetylenediide and perfluoroalkylcarboxylate for coordination sites around a silver(I) ion. A general strategy that employed $C_2@Ag_n$ polyhedra as building blocks for self-assembly of new coordination frameworks via the introduction of bridging ligands between agglomerated components then led to the isolation of a series of supramolecular complexes exhibiting distinctly different crystal structures (discrete molecules, 1D, 2D and 3D networks). Finally, attempts to distort or even disrupt the formation of polyhedral $C_2@Ag_n$ with specific ligands were explored.

8. Concluding remarks

This report provides an overview of our synthetic and structural investigations of a new family of Ag_2C_2-containing complexes, which are characterized by the existence of $C_2@Ag_n$ building units. The intramolecular Ag···Ag distances in the Ag_n aggregates fall in the range of 2.7–3.4 Å, which provide unequivocal evidence for the significance of weak closed-shell d^{10}–d^{10} argentophilic interactions. Unlike its isoelectronic diatomic analogs, C_2^{2-} exhibits a variety of bonding modes to stabilize the Ag_n cage motifs. In some cases, co-existing solvento ligands and weak interactions such as hydrogen bonding dictate the manifestation of the solid-state structures. However, due to the presence of various subtle interactions in such supramolecular systems, the crystal engineering of Ag_2C_2-containing coordination networks is still at a primitive stage and defies preconceived strategies of supramolecular assembly.

Acknowledgements

This work is supported by the Hong Kong Research Grants Council (CERG Ref. No. CUHK 4268/00P and 401704) and a Strategic Investments Scheme administrated by The Chinese University of Hong Kong.

References

[1] (a) J.A. Shaw, E. Fisher, J. Am. Chem. Soc. 68 (1946) 2745;
(b) R. Vestin, E. Ralf, Acta Chem. Scand. 3 (1949) 101;
(c) J. Österlöf, Acta Crystallogr. 7 (1954) 637;
(d) X.-L. Jin, G.-D. Zhou, N.-Z. Wu, Y.-Q. Tang, H.-C. Huang, Acta Chem. Sin. (Chin. Ed.) 48 (1990) 232, A description of the structure is given in: T.C.W. Mak, G.-D. Zhou, Crystallography in Modern Chemistry: A Resource Book of Crystal Structures, Wiley–Interscience, New York, 1992, p. 288.
[2] P. Pyykkö, Chem. Rev. 97 (1997) 597.
[3] (a) H. Schmidbaur, Gold: Progress in Chemistry, Biochemistry, and Technology, Wiley, Chichester, New York, 1999;
(b) H. Schmidbaur, Gold Bull. 23 (1990) 11;
(c) H. Schmidbaur, Chem. Soc. Rev. 24 (1995) 391;
(d) R.B. King, J. Organomet. Chem. 536 (1997) 7;
(e) O.D. Häberlein, H. Schmidbaur, N. Rösch, J. Am. Chem. Soc. 116 (1994) 8241;
(f) P. Pyykkö, Chem. Rev. 88 (1988) 563;
(g) P. Pyykkö, Y.-F. Zhao, Angew. Chem. Int. Ed. 30 (1991) 604.
[4] (a) F.A. Cotton, X. Feng, M. Matusz, R. Poli, J. Am. Chem. Soc. 110 (1988) 7077;
(b) J. El-Bahraoudi, J.M. Molina, D.P. Olea, J. Phys. Chem. A 102 (1998) 2443;
(c) M.-L. Tong, X.-M. Chen, B.-H. Ye, L.-N. Ji, Angew. Chem. Int. Ed. 38 (1999) 2237;
(d) A. Galet, V. Niel, M.C. Munoz, J.A. Real, J. Am. Chem. Soc. 125 (2003) 14224;
(e) U. Siemeling, U. Vorfeld, B. Neumann, H.-G. Stammler, Chem. Commun. (1997) 1723;
(f) J.-M. Poblet, M. Bénard, Chem. Commun. (1998) 1179.
[5] (a) H.L. Hermann, G. Boche, P. Schwerdtfeger, Chem. Eur. J. 7 (2001) 5333;
(b) E.J. Fernández, J.M. López-de-Luzuriaga, M. Monge, M.A. Rodríguez, Inorg. Chem. 37 (1998) 6002.
[6] (a) X.-M. Chen, T.C.W. Mak, Dalton Trans. (1991) 3253;
(b) O.M. Yaghi, H. Li, J. Am. Chem. Soc. 118 (1996) 295;
(c) K. Singh, J.R. Long, P. Stavropoulos, J. Am. Chem. Soc. 119 (1997) 2942;
(d) C.J. Shorrock, B.-Y. Xue, P.B. Kim, R.J. Batchelor, B.O. Patrick, D.B. Leznoff, Inorg. Chem. 41 (2002) 6743;
(e) A.N. Khlobystov, A.J. Blake, N.R. Champness, D.A. Lemenovskii, A.G. Majouga, N.V. Zyk, M. Schröder, Coord. Chem. Rev. 222 (2001) 155;
(f) G. Margraf, J.W. Bats, M. Bolte, H.-W. Lerner, M. Wagner, Chem. Commun. (2003) 956;
(g) R.D. Köhn, G. Seifert, Z. Pan, M.F. Mahon, G. Kociok-Köhn, Angew. Chem. Int. Ed. 42 (2003) 793;
(h) J.-P. Zhang, Y.-B. Wang, X.-C. Huang, Y.-Y. Lin, X.-M. Chen, Chem. Eur. J. 11 (2005) 552.
[7] (a) M.A. Rawashdeh-Omary, M.A. Omary, H.H. Patterson, J. Am. Chem. Soc. 122 (2000) 10371;
(b) M.A. Omary, T.R. Webb, Z. Assefa, G.E. Shankle, H.H. Patterson, Inorg. Chem. 37 (1998) 1380;
(c) C.-M. Che, M.-C. Tse, M.C.W. Chan, K.K. Cheung, D.L. Phillips, K.-H. Leung, J. Am. Chem. Soc. 122 (2000) 2464;
(d) P.D. Harvey, Coord. Chem. Rev. 153 (1996) 175;

(e) C.-M. Che, Z. Mao, V.M. Miskowski, M.-C. Tse, C.-K. Chan, K.-K. Cheung, D.-L. Phillips, K.-H. Leung, Angew. Chem. Int. Ed. 39 (2000) 4084.
[8] G.-C. Guo, G.-D. Zhou, Q.-G. Wang, T.C.W. Mak, Angew. Chem. Int. Ed. 37 (1998) 630.
[9] G.-C. Guo, Q.-G. Wang, G.-D. Zhou, T.C.W. Mak, Chem. Commun. (1998) 339.
[10] G.-C. Guo, G.-D. Zhou, T.C.W. Mak, J. Am. Chem. Soc. 121 (1999) 3136.
[11] Q.-M. Wang, G.-C. Guo, T.C.W. Mak, J. Cluster Sci. 13 (2002) 63.
[12] Q.-M. Wang, G.-C. Guo, T.C.W. Mak, J. Organomet. Chem. 670 (2003) 235.
[13] Q.-M. Wang, T.C.W. Mak, J. Am. Chem. Soc. 122 (2000) 7608.
[14] Q.-M. Wang, T.C.W. Mak, J. Cluster Sci. 12 (2001) 391.
[15] Q.-M. Wang, T.C.W. Mak, J. Am. Chem. Soc. 123 (2001) 1501.
[16] Q.-M. Wang, T.C.W. Mak, J. Am. Chem. Soc. 123 (2001) 7594.
[17] (a) Q.-M. Wang, T.C.W. Mak, Angew. Chem. Int. Ed. 40 (2001) 1130; (b) Q.-M. Wang, T.C.W. Mak, Chem. Eur. J. 9 (2003) 43.
[18] (a) Q.-M. Wang, T.C.W. Mak, Chem. Commun. (2001) 807; (b) Q.-M. Wang, H.-K. Lee, T.C.W. Mak, New J. Chem. 26 (2002) 513.
[19] (a) Q.-M. Wang, T.C.W. Mak, Angew. Chem. Int. Ed. 41 (2002) 4135; (b) Q.-M. Wang, T.C.W. Mak, Chem. Commun. (2002) 2682; (c) Q.-M. Wang, T.C.W. Mak, Dalton Trans. (2003) 25.
[20] X.-L. Zhao, Q.-M. Wang, T.C.W. Mak, Chem. Eur. J. 11 (2005) 2094.
[21] Q.-M. Wang, T.C.W. Mak, Inorg. Chem. 42 (2003) 1637.
[22] X.-L. Zhao, T.C.W. Mak, Polyhedron 24 (2005) 940.
[23] X.-L. Zhao, T.C.W. Mak, Dalton Trans. (2004) 3212.
[24] X.-L. Zhao, T.C.W. Mak, Polyhedron 25 (2006) 975.
[25] X.-L. Zhao, Q.-M. Wang, T.C.W. Mak, Inorg. Chem. 42 (2003) 7872.
[26] X.-L. Zhao, T.C.W. Mak, Inorg. Chim. Acta 359 (2006) 3451.
[27] X.-L. Zhao, T.C.W. Mak, Organometallics 24 (2005) 4497.
[28] X.-L. Zhao, L.-P. Zhang, T.C.W. Mak, Dalton Trans. (2006) 3141.